

This article appeared in a journal published by Elsevier. The attached copy is furnished to the author for internal non-commercial research and education use, including for instruction at the authors institution and sharing with colleagues.

Other uses, including reproduction and distribution, or selling or licensing copies, or posting to personal, institutional or third party websites are prohibited.

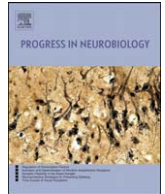
In most cases authors are permitted to post their version of the article (e.g. in Word or Tex form) to their personal website or institutional repository. Authors requiring further information regarding Elsevier's archiving and manuscript policies are encouraged to visit:

<http://www.elsevier.com/copyright>



Contents lists available at ScienceDirect

Progress in Neurobiology

journal homepage: www.elsevier.com/locate/pneurobio

A modeler's view on the spatial structure of intrinsic horizontal connectivity in the neocortex

Nicole Voges^{a,*}, Almut Schüz^c, Ad Aertsen^{a,b}, Stefan Rotter^{a,b}

^a Faculty of Biology, Albert-Ludwig University Freiburg, Germany

^b Bernstein Center Freiburg, Germany

^c Max Planck Institute for Biological Cybernetics, Tübingen, Germany

ARTICLE INFO

Article history:

Received 23 July 2009

Received in revised form 10 April 2010

Accepted 27 May 2010

Keywords:

Cortical network

Distant synapses

Patchy projections

ABSTRACT

Most current computational models of neocortical networks assume a homogeneous and isotropic arrangement of local synaptic couplings between neurons. Sparse, recurrent connectivity is typically implemented with simple statistical wiring rules. For spatially extended networks, however, such random graph models are inadequate because they ignore the traits of neuron geometry, most notably various distance dependent features of horizontal connectivity. It is to be expected that such non-random structural attributes have a great impact, both on the spatio-temporal activity dynamics and on the biological function of neocortical networks. Here we review the neuroanatomical literature describing long-range horizontal connectivity in the neocortex over distances of up to eight millimeters, in various cortical areas and mammalian species. We extract the main common features from these data to allow for improved models of large-scale cortical networks. Such models include, next to short-range neighborhood coupling, also long-range patchy connections.

We show that despite the large variability in published neuroanatomical data it is reasonable to design a generic model which generalizes over different cortical areas and mammalian species. Later on, we critically discuss this generalization, and we describe some examples of how to specify the model in order to adapt it to specific properties of particular cortical areas or species.

© 2010 Elsevier Ltd. All rights reserved.

Contents

1. Introduction	278
2. A model of horizontal cortical connectivity	279
2.1. Working assumptions	279
2.2. The generalized computational network model	279
3. Neuroanatomical basis of the model	281
3.1. Local connections	281
3.2. Intrinsic horizontal distant connections	282
3.2.1. Are patches a general feature of cortex?	282
3.2.2. Functional aspects of patchy projections	283
3.2.3. Some remarks on experimental methods: extra- vs. intracellular data	284
3.2.4. Quantitative data on patches	285
3.2.5. Overlapping patches of adjacent neurons.	286
4. Validity and specifications of the generalized model.	287
4.1. Cortical hierarchy and patches.	287
4.2. Model validity with respect to different species	288
5. Discussion	288
5.1. Basic spatial settings and local connections	288
5.2. Patches and single-cell data	289

* Corresponding author at: INSERM U751 – Université Aix-Marseille, Faculté de Médecine La Timone, 27 Bd Jean Moulin, 13385 Marseille Cedex 05, France.

Tel.: +33 491 29 98 13; fax: +33 491 78 99 14.

E-mail address: nicole.voges@univmed.fr (N. Voges).

5.3. Patches and group data	289
5.4. What we did not include	290
6. Conclusions	290
Acknowledgements	290
References	290

1. Introduction

One of the basic questions in brain research is how to model the architecture of cortical networks. To simulate cortical network dynamics, one has to assume a concrete structural substrate. Obviously, this substrate depends on the scale of the model. On the one hand, there is the macroscopic scale, describing the connectivity between different cortical areas (e.g., Hilgetag et al., 2000). On the other hand, there is the smaller scale of networks that reside within one area. In the latter case, one has to describe the connectivity between individual cells located in a confined volume of brain tissue. This is the typical scale of many cortical network models, which mimic networks that are rather small and localized, with a volume in the order of a cubic millimeter (e.g., Mehring et al., 2003; Kumar et al., 2008a).

Here, we describe neuronal connections at the network level, and consider neurons located within one cortical area as constituents of a spatially extended network within that area. The basic idea is that the geometry of dendrites and axons determines the topology of those networks, i.e., we assume that a synapse is made wherever an axon of one neuron comes close enough to a dendrite of another (Hellwig, 2000; Kalisman et al., 2003). In addition to the neighborhood couplings between closely located neurons (local), we also include more distant (non-local) connections. Reviewing the neuroanatomical literature on horizontal connectivity in the neocortex, we identify and discuss important features that should be included in models of spatially embedded cortical networks. Accordingly, we propose an exemplary model describing the intrinsic horizontal connectivity. Note that we neither consider layer-specific and white matter connections, nor cell type specific links. Our aim is to devise a general framework that reflects the basic features of lateral connectivity in

the neocortex, in particular distant connections beyond the local neighborhood of a neuron, and the feature that long-range connections established by pyramidal neurons tend to be organized in patches. The term ‘patch’ means that synapses established by a neuron or a group of neurons form spatial clusters, see Fig. 1, right and Fig. 3. Complementary to this qualitative definition, a more quantitative one of spatially clustered projection patterns can be found in Binzegger et al. (2007).

The neuroanatomical literature usually provides very specific data, validated for a certain experimental method applied in one cortical region and in one animal species. The data derived from different areas and species often shows large variations, and in most cases the reported number of measurements is too small to derive reliable statistics of the parameters in question. Moreover, there is considerable variability among different studies reporting on one area in the same species, or even in the data described within one study (see Tables 1–4). A modeler, however, has a definite need for ascertained values (or plausible ranges of values), and is interested in statistical rules characterizing the structure of the network. This is what we call the “modeler’s perspective”. Confronted with an unknown degree of specificity in cortical connectivity, we summarize these sparse and highly variable anatomical data in terms of a qualitative description of the system, resulting in a generic model. To this end, we review the literature concerning horizontal cortical connectivity, compare data obtained with different experimental methods from distinct areas and species, and extract their common features. This allows us to come up with plausible assumptions on typical values, and to assess upper and lower bounds for the latter. Naturally, such an approach yields a model that characterizes key aspects of horizontal connectivity but cannot account for brain area- or species-specific details. Therefore, in a second step, we elaborate

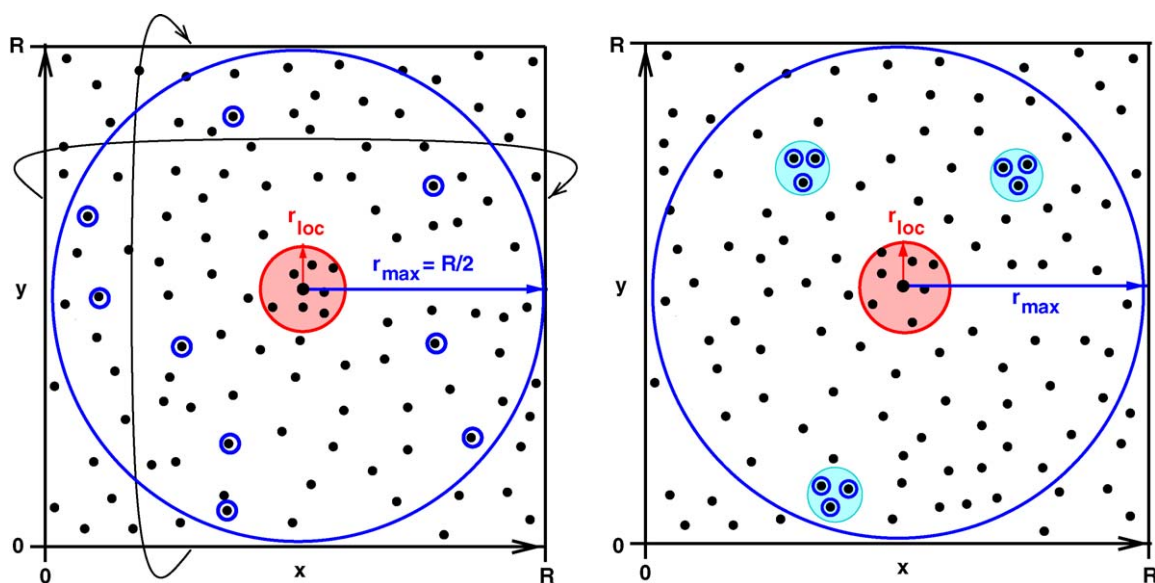


Fig. 1. Network model comprising spatially embedded pyramidal neurons (black dots) with both local (red) and long-range (blue) connectivity. Surface view of a 2D sheet of neocortex. Neurons connected to the center neuron are represented by open blue circles. Left: Uniformly distributed distant projections. Right: Clustered long-range connectivity. Cyan disks represent patches.

on our generalization: we depict some specificities, and suggest the appropriate modifications of the generalized model to adapt it to the details deemed important. This is the typical strategy of modeling: one starts with as simple a model as possible (capturing the essentials of the system in question), while more complex features are added only in additional steps.

Searching the literature for data on horizontal patchy connections in the neocortex, we encountered a number of very helpful reviews: Levitt and Lund (2002) describe and compare the patchy connections in different areas and species, an issue that is also part of Elston (2007) and Douglas and Martin (2004). Lewis et al. (2002) focus on the connectivity in the macaque prefrontal cortex with regard to the spatial distance of the connected neurons. Additionally, Angelucci and Bressloff (2006), Lund et al. (2003), Schmidt and Löwel (2002), and Gilbert (1992) discuss this topic in relation to functional aspects of cortical connections in the visual cortex. These studies indicate that the spatial component of cortical connectivity indeed plays an important role for cortical function.

Previous models of cortical networks employed to understand cortical activity dynamics frequently assumed purely random connectivity (e.g., van Vreeswijk and Sompolinsky, 1996, 1998; Brunel, 2000), similar to random graphs (Erdős and Rényi, 1959). More realistic models of local cortical networks take the spatial domain into account: Mehring et al. (2003) and Kumar et al. (2008b) consider distance dependent couplings between neurons co-located within the range of a cortical column. Voges and Perrinet (2010) showed that including distance dependent conduction delays induces significant changes in the dynamical phase space. The studies by Kaiser and Hilgetag (2004a,b) provide further models of spatially embedded networks. Other, more abstract analyses of cortical connectivity, dealing with wiring optimization and scaling laws in the cortical network (Braitenberg, 2001; Karbowski, 2003; Chklovskii, 2004) ask questions like: What would be the model that minimizes the amount of wiring (total length of dendritic and axonal arborizations) combined with the most effective connectivity (minimal number of steps to connect any pair of neurons, the average shortest path length)? The small-world network (Newman, 2003) provides an interesting near-optimal solution (Sporns and Zwi, 2004; Buzsaki et al., 2004; Bassett and Bullmore, 2006; DeLosRios and Petermann, 2007), based on the assumption that most synapses are established locally, and that a rather limited number of long-range connections enable information transfer between distant neurons.

As the present study represents the view of a modeler, we start off in Section 2 with the development of our cortical network model. We list the prerequisites necessary to set up a spatially extended cortical network, and introduce the pertinent parameters. In Section 3, we present a classification scheme of distance dependent connectivity in the cortex. Within this scheme, our focus on horizontal patchy connections is elucidated. We review the corresponding neuroanatomical literature, and extract the numerical values for our model parameters. In Section 4, we suggest some specific adjustments of the generic model devised in Section 2. Finally, we discuss our model in the light of the anatomical data presented in Sections 3 and 4.

2. A model of horizontal cortical connectivity

As suggested by its title, this article attempts to relate neuroanatomical findings on cortical connectivity specifically to a modeler's needs. For this reason we start with a presentation of our generalized model for horizontal connectivity in the cortex. The advantage of this procedure is that we define in advance which type of quantitative data is required, before diving into the details of neuroanatomical facts and findings. We first state the

requirements adopted for the development of the model, our working assumptions, and then present our model.

2.1. Working assumptions

Our aim is to come up with a model of intrinsic horizontal synaptic connections in the neocortex. Axons traveling through the white matter are not considered here. It is assumed that, based on axonal and dendritic ramifications, neuronal morphology defines network topology. For neurons embedded in physical space, this suggests distance dependent connectivity profiles (Chklovskii et al., 2002; Kalisman et al., 2003; Hellwig, 2000). Here, we discuss quasi two-dimensional domains with an area of approximately half a square centimeter. Thus, we consider a multiple of the one square millimeter that is thought to correspond in some locations to a functional column, studied in many network models (e.g., Kumar et al., 2008a). This makes it necessary to capture the non-local connections of pyramidal cells, especially the distant patchy projection patterns.

In general, we take a statistical approach assuming random couplings, the probabilities of which are constrained by neuroanatomical data. Moreover, our viewpoint is influenced by additional considerations, particularly with respect to wiring economy. In our generic model, we assume (statistically) isotropic connectivity profiles that are identical for all neurons. On average, every neuron has the same number of incoming and outgoing synapses that are equally distributed among local and distant projection targets, respectively.

The current version of our model neglects the layered structure of the cortex, as well as any layer specific connectivity. Thus, we consider a planar sheet of neurons with all six cortical layers condensed into one. Alternatively, only a subset of layers is represented, e.g., layers 2/3. For possible modeling perspectives to relax this simplification by considering multiple layers, see Krone et al. (1986) and Kremkow et al. (2007) for the primary visual cortex. Several excellent reviews describe the connectivity within and across cortical layers (e.g., Thomson and Bannister, 2003; Binzegger et al., 2004; Bannister, 2005).

2.2. The generalized computational network model

We consider 80–85% of the neurons to be excitatory, all represented by pyramidal cells (but including spiny stellate cells) and 15–20% of the neurons to be inhibitory interneurons. These values have been found in cats (e.g. Gabbott and Somogyi, 1986), primates (e.g. Braak and Braak, 1986; Jones et al., 1994), and rodents (e.g. Peters et al., 1981; Beaulieu, 1993), possibly with a slight dependence on brain size (see Hornung and De Tribolet, 1994): the fraction of inhibitory neurons reported for rodents are at the lower end (around 15%). A first question is how to position pyramidal cells in space, at random or in a grid-like fashion? A similar question concerns the inhibitory interneurons: How to distribute them among the excitatory pyramidal cells? Based on earlier work (Voges et al., 2007), we propose to distribute pyramidal cells randomly and independently with uniform density, but to place the interneurons on jittered grid positions. Doing so keeps the interneurons at a minimum distance, whereas pyramidal cells may sit on top of each other. This projection artefact must be expected as a direct consequence of our 2D layout.

In any concrete realization of a model network, the number N of neurons we can handle for numerical or combinatorial network analysis is limited, due to computational constraints. This forces us to accept neuron densities far below any realistic value. For example, in the brain of the mouse, there are about 90,000 neurons per cubic millimeter of cortical tissue (Schüz and Palm, 1989). A square patch of mouse cortex of side length $R = 8$ mm (see below)

and as thick as layers 2/3 (approximately 250 μm) has a volume of about 16 mm^3 . It thus contains a total of about 1.4 million neurons, which is clearly beyond what we can currently handle on our computers. Given $N = 100,000$ neurons, a network size we can handle, our model yields a density of only 6250 neurons per cubic millimeter.

Another issue are boundary effects, due to the finite domain considered here. We circumvent these by forming a torus out of the square, imposing periodic boundary conditions. As a result, $r_{\text{max}} = R/2$ is the radius of the largest circle in our network that does not overlap with itself. In the model, we distinguish two separate connectivity profiles, which characterize the projection types of a neuron located in the center of these profiles:

- Local synaptic connections, established with neurons located within a circular neighborhood of radius r_{loc} (red circle in Fig. 1). Within this local-range we assume a uniform connection probability p_{loc} .
- More distant synaptic connections, established with neurons outside the local range, provided their distance is not larger than r_{max} (large blue circle in Fig. 1). Depending on the model for these distant projections, one could again assume uniformly distributed terminals, where any potential connection between the neuron in the center and a neuron at distance r in the ring

$r_{\text{loc}} < r < r_{\text{max}}$ is established with the same probability (Fig. 1, left). Alternatively, one might assume spatially clustered, patchy termination fields of the projections. In this case, the central neuron establishes links to distant localized groups of neurons (Fig. 1, right).

As a next step, we need to set the model parameters to specific values. For now, we give *ad hoc* value, justify them later in Section 3, and discuss them in Sections 4 and 5. The network has N neurons, embedded in a 2D square area of side length $R = 8$ mm, rolled up to a torus. The largest circular neighborhood fitting into this domain has a radius of $r_{\text{max}} = 4$ mm. All local connections remain within a circular domain of radius $r_{\text{loc}} = 0.5$ mm. We assume that, on average, each neuron has the same (average) number k of incoming and outgoing links. This leads to a global connectivity $c = k/N$, composed of both local and distant synapses. The relative proportion of local versus long-range projections is, in fact, a very important characteristic of the network. For inhibitory neurons we assume only local connections. In contrast, each of the pyramidal cells in our model establishes 60% of its synapses locally while the other 40% target neurons that are more than $r_{\text{loc}} = 0.5$ mm away from the cell body.

In addition to its local projections, each pyramidal neuron establishes $N_p = 3$ distant circular patches, each with a radius

Table 1
List of publications on patchy projections resulting from extracellular tracer injections ('group data', focused on anterogradely labeled fibers), ordered according to the species brain size and cortical areas.

Literature	Species	Cortical areas	σ	N_p	θ_p	d_p	$d_{p_{\text{max}}}(\Sigma)$	d_{cc}
Burkhalter and Bernado (1989)	human	V1, V2	0.25–1		0.3–0.5	1–2	6	0.6–1
Galuske et al. (2000)	human	22, A1 (intr.)	0.4	10–58, 30–50	0.56–0.86, 0.39–0.43		7, 5	1–1.5, 0.87–0.95
Huntley and Jones (1991)	macaque	motor cortex	0.8–1.1		0.5–1		7–8	small gaps
Pucak et al. (1996)	monkey	PFC	0.35	12	0.25	2.8	7.5 (9.5 \times 5)	
Levitt et al. (1993)	macaque	PFC (intr.)	0.2–0.4		0.2–0.4		7–8	0.5–0.6
Lund et al. (1993)	macaque	PFC (intr.)	0.2, 0.3–1.5	>30	0.27		(9.4 \times 3)	0.54
Lund et al. (1993)	macaque	V1,2,4 (intr.)	0.2, 0.3–1.5	>30	0.23, 0.34(5)		3,4,6	0.43, 0.64(8)
Lund et al. (1993)	macaque	SI (1 intr. & to 3b, 2)	0.2–0.39	>30	0.27 \times 0.39, 0.3 \times 0.45		(7 \times 6, 4.7 \times 5)	0.75, 0.54
Lund et al. (1993)	macaque	motor (4, intr.)	0.25, 0.42	>30	0.48		(6 \times 5, 7.4 \times 5)	0.85
Amir et al. (1993)	macaque	V1,2, 4,7a (intr.)	0.13–0.9	V1: 5–11, V4: 15–33	0.23, 0.25, 0.31, 0.27	0.65–2.21	2.14–8.98	0.61, 1.15, 1.4, 1.56
Levitt et al. (1994)	macaque	V2 (intr.)	0.2–0.3	10–15	0.25–0.3	2	4	0.25–2.2
Rockland and Lund (1983)	macaque squirrel	V1 (intr.)	0.5–0.75		0.2		1.5, 3	0.5–0.6, 0.35–0.45
Stettler et al. (2002)	macaque	V1 intr., (V2 to V1)	0.2		0.25	0.5–3.5	(7)	0.75 (0.5)
Tanigawa et al. (2005)	macaque	V1, TE	0.23–0.54	5–21, 9–43	0.25 \times 0.39 0.35 \times 0.55	0.9–2, 2.5–7.7		
Fujita and Fujita (1996)	macaque	TE, TEO	0.2–0.5	7–20, 25	0.4–0.6, 0.35–0.45		4 (7.3 \times 4.6)	0.2–1.56, 0.39–1.42
Yoshioka et al. (1996)	macaque	V1	0.1–0.21	3–17	0.1–0.25		(1.6–3.7)	
Yoshioka et al. (1992)	macaque	V4	0.25	3.8/ mm^2	0.25–0.45	0.5–3.5		0.45–1.3
Malach et al. (1997)	owl monkey	V5 (intr.)	0.15–3.5	>29	0.3–0.5			max =1.8
Malach et al. (1994)	squirrel monkey	V2	0.1–0.4		0.23–0.38		(4–5)	0.6
Sincich and Blasdel (2001)	squirrel,owl monkey	V1	0.2–0.3		0.2	1	1.5	
Buzás et al. (2006)	cat	visual	0.15		0.25	1.2, 2.1	3	
Kisvárdy et al. (1997)	cat	V1, V2	0.15, 0.08	20, 15	0.2–1, mostly 0.5–0.6		2.5, 3.5	0.9 1.2
Luhmann et al. (1986)	cat	V1	1–2.5		0.2–0.4	0.7–1.7	3.5	0.4–0.8
Wallace et al. (1991)	cat	A1		3–8	0.8–2	0.5–4	6	1
Wallace and Bajwa (1991)	ferret	A1 (intr.)	0.3–1	6–8	0.3–0.8	0.5–4		
Rockland et al. (1982)	tree shrew	V1 (intr.)	0.5, 1.5		0.75–1 \times 0.23–0.25		3	0.5
Bosking et al. (1997)	tree shrew	V1 (intr.)	0.2		0.2 \times 0.4	>0.5		
Burkhalter and Charles (1990)	rat	V1, V2	0.1–0.25		0.15–0.25		1.8	
Rumberger et al. (2001)	rat	V1, V2 (intr.)	0.3–0.6	1–3	0.37, 0.43, 0.46			0.75, 0.9

Listed are the injection size σ (diameter), the average number of patches per injection N_p , the average patch diameter θ_p (or stripe width), the average and maximum lateral distance between the injection site and its patches d_p , $d_{p_{\text{max}}}$, the maximum lateral axonal spread Σ , and the average distance between the patches d_{cc} . All length measurements are given in millimeters.

$r_p = r_{loc}/2 = 250 \mu\text{m}$ (diameter $\varnothing_p = 0.5 \text{ mm}$), see Fig. 1, right. The position of a patch is defined by its angle Φ and its radial distance d_p from the neuron in the center, as shown in Fig. 3. One also needs to fix the spatial arrangement of the patches emerging from different neurons. Again, there are several possibilities: patches of different neurons could be independently positioned or, alternatively, different neurons could have patches that overlap to a degree that depends on the distance between the source neurons.

Obviously, the choice of a specific patch model will substantially influence the overall topology of the network. Inspired by data from extracellular tracer injection studies (cf. Table 1) we propose the following simplified description: distant projections emerging from a group of neurons located in a compact spatial region are confined to six common potential patch positions. Individual neurons find their targets in $N_p = 3$ out of the 6 possible positions, chosen randomly, see Fig. 4. These compact spatial regions represent the local extent of extracellular staining surrounding the injection site, while each patch corresponds to a clustered distant projection. In our model, we conceive these compact regions as quadratic boxes with side length $bl = 0.5 \text{ mm}$, see Fig. 4. For each of these boxes we specify six random patch positions. The distances from the box center to each patch d_p are chosen from the interval $[r_{loc} + r_p, r_{max} - r_p]$, corresponding to $[0.75, 3.75] \text{ mm}$ in our case.

Other important quantities directly follow as a consequence of the assumptions described above, e.g. the number of connections established by a neuron to the neurons located within one patch, or the amount of common input to all neurons located within one patch. For example, in case of 60% local connections, a neuron has on average $0.6 \times k$ local synapses and approximately $0.6 \times 0.33 \times k$ links with the neurons located within one distant patch. Another derived quantity is the inter-patch distance d_{cc} .

So far, we adopted *ad hoc* parameter values. In the following section we will explain why we chose these parameter values, relating them to the available neuroanatomical data.

3. Neuroanatomical basis of the model

For the sake of simplicity, we distinguish in this model three types of connections, according to their spatial range (colors refer to the two schemes displayed in Fig. 2):

- Local synapses, established by the local axon collaterals (red) of pyramidal cells (PC) and inhibitory interneurons (not shown). They usually arborize within a distance of up to $500 \mu\text{m}$ from the cell body.
- Intrinsic horizontal distant connections (blue) of pyramidal cells. These are made by axon collaterals traveling through the gray

matter in parallel to the surface, over distances of up to several millimeters, usually with neurons within the same cortical area.

- Extrinsic long-range projections of pyramidal cells (black). The main axon passes through the white matter to establish synapses with neurons over still larger distances, usually in another cortical area.

Although transitions between these systems exist (Schüz et al., 2005) this classification scheme is well justified by the morphological characteristics of pyramidal cells. The literature provides examples of a similar classification for the monkey prefrontal cortex (e.g., Lewis et al., 2002; Melchitzky et al., 1998, 2001). Likewise, McGuire et al. (1991) distinguish between proximal and distal collaterals in the macaque primary visual cortex, and Ojima et al. (1991) describe an intra-areal connectivity system, composed of local and additional long-range links in the cat auditory cortex. For more examples, see Section 3.1.

In the present paper, we do not (explicitly) include white matter projections. Instead, we focus on the first two systems, the local and the intrinsic horizontal distant projections. (For a quantitative study on white matter connections see Schüz and Braitenberg, 2002).

3.1. Local connections

We propose to set the local connectivity range in the model to $r_{loc} = 500 \mu\text{m}$, which is the upper limit found in the literature. In macaque prefrontal cortex (PFC) Levitt et al. (1993), Lewis et al. (2002), and Melchitzky et al. (2001) assessed $r_{loc} \sim 300 \mu\text{m}$. Likewise, in Ojima et al. (1991, cat A1) and Yabuta and Callaway (1998, macaque V1) r_{loc} came out about $300 \mu\text{m}$, whereas in Burkhalter and Charles (1990, rat V1,2), Kisvárdy et al. (1986, cat aerea 17), Kisvárdy and Eysel (1992, cat area 17), Bosking et al. (1997, tree shrew V1), Stettler et al. (2002, macaque V1) and Malach et al. (1993, macaque V1) it was estimated as $400\text{--}500 \mu\text{m}$.

The distinction between local and non-local intrinsic connections is mainly based on the morphology of the axonal tree, as evident from single cell reconstructions. Axon collaterals that ramify within and around the region of the dendritic tree are considered to be of short, local range. Horizontally running collaterals that branch beyond this range establish non-local, intrinsic projections (Ghosh et al., 1988, cat 4 γ ; Ghosh and Porter, 1988, macaque motor cortex; Lohmann and Rörig, 1994, rat V2). The axonal arborizations for $r < r_{loc}$ tend to be homogeneous (Kisvárdy et al., 1986, cat aerea 17; Ojima et al., 1991, cat A1; Malach et al., 1993, macaque V1), while the projection patterns for distances larger than r_{loc} tend to be clustered. In most tracer

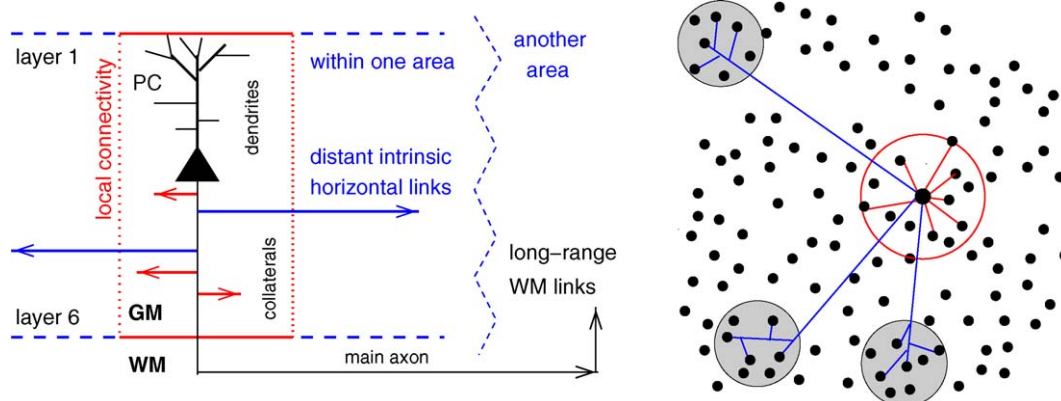


Fig. 2. Scheme illustrating the types of projections made by pyramidal cells (PC). Local connections are shown in red, horizontal distant projections within the gray matter (GM) in blue. Left: Lateral view including the white matter (WM) projections shown in black. Right: Top view onto a sheet of cortex with embedded PCs (black dots) and their patchy axonal ramifications. The gray disks represent patchy projection sites.

experiments, these two kinds of projections are obvious. In studies using extracellular tracer injections (e.g. Burkhalter and Charles, 1990, rat V1.2; Amir et al., 1993, macaque visual cortex; Levitt et al., 1993, macaque PFC; Malach et al., 1993, macaque V1, Malach et al., 1997, squirrel monkey V2; Schüz et al., 2005, mouse neocortex), the local range $r < r_{loc}$ corresponds to the fiber range constituting the halo around the injection site, while for $r > r_{loc}$ there is a tendency towards spatially clustered fiber accumulations (although this is less evident in small brains, see Sections 3.2.1 and 4.2).

Another criterion is based on functional aspects, see Section 3.2.2. In the visual cortex, projections further than 400–500 μm have been found to have a tendency to interconnect regions of similar orientation selectivity, whereas fibers within a range of about 400 μm did not show a selective projection pattern (Bosking et al., 1997, tree shrew; Stettler et al., 2002; Malach et al., 1993 in macaque V1). Yet, Mooser et al. (2004) reported an orientation specific bias also in the local arrangement of feedforward connections from layer 4 to layer 2/3 in V1 of the tree shrew. The resulting values for r_{loc} are consistent with studies dealing with local connections explicitly (Hellwig, 2000, rat visual cortex; Budd and Kisvárdy, 2001, cat area 17; Holmgren et al., 2003, rat visual & somatosensory cortex; Stepanyants et al., 2007, cat area 17).

The proportion of local versus distant projections of a PC is not well known. Based on tracer injections, Schüz et al. (2005) estimated for the mouse cortex that at least fifty five percent of the total axonal length of a pyramidal cell consists of local ramifications (excluding in this calculation the axon in the white matter, but including callosal or other distant cortical terminal fields). It is possible that in the small brain of the mouse the local connectivity is relatively higher than in larger brains: In a recent study on cat area 17 Stepanyants et al. (2009) found only 26% of the excitatory synapses within a cylinder with a radius of 500 μm to come from neurons located within that volume, the remaining synapses coming either from distant intrinsic connections or from more distant places via the white matter. Ojima et al. (1991, cat A1) mention that there are more local than distant intrinsic axon collaterals (approximately 3:1). Kisvárdy and Eysel (1992, cat area 17) counted the boutons made by axon collaterals and found twice as many boutons in the local range compared to the distant intrinsic range. The latter two studies do not include distant connections via the white matter - which are also not captured in our model. From these two studies, we conclude that a range of 60–75% intrinsic local as compared to intrinsic distant connections is a reasonable estimate for our model. It is interesting to relate these results to the data by Stepanyants et al. (2009, see above). If we assume that approximately half of the synapses of a PC originate from extrinsic projections via the white matter, our lower boundary of 60% local intrinsic connections (as compared to 40% synapses in the patches) would correspond to 30% local connections in total, which is close to the 26% given in Stepanyants et al. (2009).

Based on the assumption that almost-touching axons and dendrites will actually form a synapse with high likelihood, Hellwig (2000) performed parametric fits for distance-dependent connectivity profiles using 3D reconstructed neurons. For layer 2/3 pyramidal cells in the rat visual cortex, he obtained Gaussian profiles with a peak contact probability of about 0.8, and a contact probability of 0.1 for cells at a distance of 500 μm . Holmgren et al. (2003), by contrast, reported relatively small values for both the range (up to 140 μm) and the probability of local connections ($p_{loc,max} \sim 0.1$ for PC-PC connections, $p_{loc,max} \sim 0.55$ for connections from PCs to inhibitory interneurons) in rat visual and somatosensory cortex. Stepanyants et al. (2007) demonstrated a strong decrease of the coupling probability with distance, for

various types of neurons in the rat visual cortex. Again, the quantitative data vary, but it is universally found that the spatial profiles of local connections decline with increasing distance.

We do not deal with cell-type specific connectivity. Nevertheless, attention should be paid to the fact that – also in terms of purely distance-dependent projections – the local connectivity profile depends on the ramification patterns of both the pre- and the postsynaptic cells involved (Stepanyants et al., 2007; Holmgren et al., 2003). For example, various kinds of interneurons have a stronger tendency to couple to their neighbors, due to their dense axonal ramifications, and in most cases, their spatial range is shorter than that of PCs (Braitenberg and Schüz, 1998; Binzegger et al., 2007; Kisvárdy et al., 1997). Here, we therefore only consider their contribution to the local connectivity system. Another example is the variation in shape and density of dendritic and axonal arbors of pyramidal cells in different layers and different cortical areas (Cajal, 1911). As described by Amirkian (2005) and Kalisman et al. (2003), it is possible to derive cell specific local connectivity profiles directly from neuronal morphologies, provided that the database is large enough.

3.2. Intrinsic horizontal distant connections

In contrast to the local connections just described, distant intrinsic horizontal projections can range up to several millimeters. They mainly connect neurons located within the same cortical area, but may also cross areal boundaries, as shown for example for the boundary between V1 and V2 (Rumberger et al., 2001; Malach, 1989, in rats; Burkhalter and Bernardo, 1989 in humans), or between areas MT and MTc (Malach et al., 1997, owl monkey).

In our network model, it is presumed that all pyramidal cell synapses established between remote neurons are part of patchy projections. The following sections elucidate various aspects of spatially clustered projections and demonstrate some evidence for this assumption. Moreover, we argue that these patchy projection patterns were observed for both groups of neurons and single cells, and we place particular emphasis on the investigation of their relation to each other (see also Voges et al., 2010). Finally, we provide a compilation of the model parameters and the associated numerical values extracted from neuroanatomical studies, ending in a discussion of the potential overlap of the terminal fields of adjacent neurons.

3.2.1. Are patches a general feature of cortex?

The existence of patchy PC projections is well-established in various cortical areas in various species, see Tables 1–4. Yet, it remains unclear whether patches are typical for most PCs, or whether they are common only for a fraction of PCs, e.g. in particular cortical areas and/or in specific species. According to Binzegger et al. (2007), clustered projections are indeed a fundamental property of spatial bouton organization in cat area 17, not only for pyramidal cells, but also for inhibitory neurons. The distinction between local and distant patchy connections would then be somewhat artificial. What we call “local connectivity range”, appears in their work as one out of several equivalent patchy projections of a neuron. Then again, Yabuta and Callaway (1998) found evidence for two distinct pyramidal cell types in macaque V1: the majority of PCs in layer 2/3 contributed to the long-range clustered projection pattern while one fourth of them did not. Clarke et al. (1993) reported even five distinct types of axons in cat A1, some of them sustain the patchy pattern of intrinsic connectivity in cat A1, whereas others do not.

As already stated, we do not deal with projections between cortical layers. Nevertheless, in the context of this section it is important to mention that patchy projections are especially

prominent in layers 2/3 and also occur in layer 5. This holds for all areas and species investigated. They have also been reported for layer 4 (Gilbert and Wiesel, 1983; Martin and Whitteridge, 1984; Kisvárdy et al., 1989; Yousef et al., 1999; Binzegger et al., 2007; all in cat area 17) and layer 6 (Gilbert and Wiesel, 1983, cat area 17; Burkhalter and Bernardo, 1989, human V1,2; Rockland and Knutson, 2001, macaque V1), but clearly less frequently than for layer 2/3.

In principle, patchy connectivity between distant sites is highly economic in minimizing the length of necessary fibers (Chklovskii, 2004; Voges et al., 2010). Due to space limitations in the brain, this is an important advantage (Chklovskii, 2000, 2004; Buzsáki et al., 2004; Bassett and Bullmore, 2006; DeLosRios and Petermann, 2007). The first step in wiring up a large network is neighborhood coupling, which can be accomplished with short cables. As already mentioned in Section 1, many synaptic 'hops' would then be necessary to connect distant neurons (high characteristic path length). A more economic solution is to allow for a few distant links, resulting in a moderate increase of the wiring length, but considerably shorter path lengths. The development of patchy distant projections constitutes an even better solution: One single long-range axon connects to several distant neurons located next to each other (within a patch). This saves fibers, while allowing for short characteristic path lengths. Such an effect is particularly important in larger brains where the distance between two connected neurons situated in different cortical areas can be comparably large.

In a small animal like the mouse, our distance-dependent connectivity scheme does not appear to be very adequate (Schüz et al., 2005): after tracer injections it can be seen that main axons often do not enter the white matter, but travel within layers 5/6. In addition, densely stained patches exist within extended terminal fields of low density, so that the local system is often not clearly separable from the distant one. In fact, in the mouse cortex it seems impossible to decide to what degree projections of up to a few millimeters away from the injection site correspond to the intrinsic distant projections in larger brains, or rather to their extrinsic white matter system. In contrast to small cortices, extracellular tracer injections in larger brains, e.g. of the monkey, result in more, well-defined patches, clearly separated from each other and from the local system, e.g. see Amir et al. (1993, macaque visual cortex). Section 4.2 provides further details on the patterns of connectivity in different species.

Another question is whether feedback connectivity (from higher cortical areas to more peripheral ones) exhibits a similar spatially clustered projection pattern. In this regard, most published studies deal with the visual cortex. For the macaque monkey Angelucci et al. (2002a,b) reported patchy feedback connections from areas V2 and V3 to V1, distributed over a large spatial region, and Rockland and Virga (1989) showed that terminations of widespread axons originating in V2 are organized in clusters in V1. Likewise, Burkhalter and Charles (1990, rat) and Burkhalter and Bernardo (1989, human) mentioned patchy feedback connections from V2 to V1. Shmuel et al. (2005, owl monkey) found that feedback projections from V2 to V1 are clearly more diffuse than intrinsic V1 connections but are definitely clustered. Rockland and Knutson (2000, squirrel monkey) showed two patterns of area MT feedback terminations to V1 and V2, even for a single axon: one with grouping in small clusters, the other one non-patchy, both forming large termination fields. Similar findings are presented in Rockland (2004a) for feedback projections from V2 to V1. Stettler et al. (2002, macaque) also report spatially widespread, highly divergent V2 to V1 feedback connections, and they stated that these connections were clearly less patchy and more diffuse than those from V1 to V2. Likewise, Anderson and Martin (2006, macaque) found that feedback connections from

area V4 to V2 seldom form patches. On the whole, these findings appear to be contradictory, although most results do indicate patchy feedback projections. In Angelucci and Bressloff (2006) some of these studies are reviewed in relation to their own results which show again spatially clustered feedback connections to V1 in old and new world primates. They discuss the possibility that the finding of non-patchy feedback might be ascribed to the experimental methods, as, for example the anatomical tracer used to visualize the projection patterns.

To recapitulate: patchy PC projections exist in a variety of cortical areas and species. They constitute an effective and economic connectivity scheme, and are presumably adapted to the functional requirements of these areas.

3.2.2. Functional aspects of patchy projections

There are several indications that patchy projections subserve special functional adaptations. Again, most published data deals with the visual system. For example, in the primary visual cortex of several species long-range patchy connections were shown to be preferably established between domains of neurons with similar orientation preference (e.g. Bosking et al., 1997 and Chisum et al., 2003 in tree shrews; Gilbert and Wiesel, 1989; Malach et al., 1993, and Stettler et al., 2002 in the macaque, Buzás et al., 2006 in cats). In addition, there are indications that the anisotropic projection patterns (see Section 4) exhibit axial specificity, i.e., a larger spatial extend and more synaptic boutons along the axis in visual space that corresponds to the preferred orientation of the injection site (see above and Sincich and Blasdel, 2001, new world monkey; Mooser et al., 2004, tree shrew). Similarly, Malach et al. (1997, owl monkey) found a tendency for intrinsic connections to connect to functional domains of similar orientation preference for areas MT and MTc, although there was a strong variation for individual cases. Yet, there are some studies in cats that report only weak (Kisvárdy et al., 1997, areas 17, 18) or no (Yousef et al., 1999, layer 4 of area 17) or even negative (Matsubara et al., 1987, area 18) correlations between lateral connectivity and orientation selectivity.

Moreover, neurons in the visual cortex are also arranged with respect to other functional specializations, e.g., mono- versus binocularity, contrast sensitivity, or ocular dominance. Cytochrome oxidase (CO) staining offers a possibility to investigate the relationship between such functional domains and lateral connections in macaque monkeys (Livingstone and Hubel, 1984; Tootell et al., 1988; Ts'o et al., 1990): cells in the CO-rich blobs in V1 are largely monocular, orientation-nonspecific, color-specific, show high contrast sensitivity, and prefer low spatial frequencies.

It has been shown that neurons in CO-blobs have a tendency to target other CO-blobs while those in interblobs target preferably other interblob regions (Yoshioka et al., 1996; Yabuta and Callaway, 1998). In V2, however, Malach et al. (1994) could not find a simple rule that describes the relationship between CO regions and intrinsic connections in V2. Concerning the visual system there are some excellent reviews (Gilbert, 1992; Angelucci and Bressloff, 2006; Schmidt and Löwel, 2002). In particular, Angelucci and Bullier (2003) and Angelucci and Bressloff (2006) discuss the contribution of feedforward, intrinsic lateral, and feedback connections to the receptive field of primate V1 neurons (see also Lund et al., 2003; Angelucci et al., 2002a,b). Intrinsic lateral connections are suggested to underlie contrast dependent changes and modulatory effects in the *near* surround receptive field. Beyond this region, clustered feedback projections are the most likely substrate for the *far* surround suppression due to their large spatial spread (see Section 3.2.1, corresponding to a large extent in visual space), and their fast conduction velocity compared to intrinsic connections (Bringuier et al., 1999, cat area 17; Yoshimura et al., 2000).

Yet, there are also some studies analyzing the organization of intrinsic (patchy) connections with respect to the functional

properties of neurons in non-visual cortical areas. Read et al. (2001), for example, showed that patchy connections in the primary auditory cortex of cats are preferentially established between subregions with similar frequency characteristics. This relationship was roughly confirmed by Wallace et al. (1991, cat A1). Ojima and Takayanagi (2004, cat A1), however, reported a small amount of overlap between the distant patchy projections of two different frequency domains. They state that this does not disprove the previous findings, but rather serves the spectral integration of sound components. Another example of connections between clusters of cells with similar response properties can be found in the somatosensory cortex of monkeys: Juliano et al. (1990, areas 3b, 1, 2) found that patchy terminal fields in areas 3b, 2 and 1 of projections from areas 1 and 3b were largely colocalized with patches of metabolic activity evoked by somatosensory stimulation and stained with deoxyglucose. An exception were the fiber terminals from area 1 to 3b. Further on, Huntley and Jones (1991) investigated the relationship of intrinsic connections to forelimb movement representations in monkey motor cortex. They concluded that the extensive horizontal collaterals provide inputs to many different movement representations and may be recruited to synchronize forelimb muscle groups. Moreover, Lewis et al. (2002) discussed the hypothesis that the sustained firing of clustered feed-forward PC connections in the prefrontal cortex is critical for working memory.

To make the case that patchy long-range projections are the common case rather than the exception, we now review the neuroanatomical data in more detail.

3.2.3. Some remarks on experimental methods: extra- vs. intracellular data

Most studies observing and analyzing patchy projections were based on in vivo extracellular injections of neuronal tracers. In this study, we focus on anterograde tracers, i.e. tracers which are taken up by the neurons at the injection site and transported to their axon terminals (e.g. Ojima and Takayanagi, 2004; Malach et al., 1993; Tanigawa et al., 2005; Rockland and Knutson, 2001). These studies showed that synapses established by localized groups of neurons were not homogeneously distributed, but appeared clustered in patches, here called 'group patches'. Table 1 provide a (non-exhaustive) list of papers presenting such data. We also list the injection size σ (diameter of the region within which the neurons are supposed to have taken up the tracer) and the measurements of several patch parameters provided by these studies: average number of patches N_p per injection, average patch diameter θ_p , average distance from the cell body to the patch d_p , average inter-patch distance d_{cc} , and total spatial spread of the axonal ramifications Σ .

Patchy projection patterns have also been shown using retrograde tracers, i.e. with the tracer taken up by axon terminals and transported back to the soma, or by employing a combination of both (Burkhalter and Charles, 1990; Pucak et al., 1996; Huntley and Jones, 1991). Retrogradely stained patches indicate that a localized group of neurons receives synapses from several, spatially clustered distant groups of neurons. Table 2 gives a

short list of studies analyzing retrogradely stained projection patterns. In fact, various neuronal tracers (e.g. biocytin, WGA-HRP, dextran amine) have both retro- and anterograde properties. Which direction is used experimentally depends on the details of the procedure and the focus of the study.

These group data can, however, not be directly interpreted with respect to ramification patterns of single neurons. Neither can it be easily inferred how many of the stained neurons actually contribute to the clustered projection pattern, nor can it be reconstructed how the fibers of a PC ramify within a patch. Moreover, it remains unclear how many patches an individual neuron contributes to or, vice versa, how many neurons contribute to an individual patch. Evidently, from the modeler's perspective, these are important issues. Buzás et al. (2006) put particular emphasis on comparing single-cell data with population data. Analyzing the relation between distance-dependent connectivity and orientation selectivity in the cat visual cortex, they found that connectivity rules defined at the population level were not necessarily valid for individual neurons.

Data on the ramification patterns of individual axons are relatively sparse, due to the more demanding experimental procedures. These procedures include the intra- or juxtacellular injection of the tracer, the 3D reconstruction of the neuron, usually over many adjacent sections, and the danger of incomplete filling of distant branches (discussed in Ghosh et al., 1988). For experimental details we refer to Buzás et al. (1998) and the reviews by Rockland (2002, 2004b). New techniques, mostly built on enhanced viral tracing methods, promise to be helpful for future research. Of particular interest is a visualization of the arborizations of few neighboring neurons in order to investigate their interactions. This type of data necessitates a simultaneous but separate staining of these neurons, e.g. using different colors. New techniques from molecular biology offer such multicolor labeling (e.g. Lichtman et al., 2008), as well as particularly sensitive staining methods (e.g. Matsuda et al., 2009; Wickersham et al., 2007). They can also be used to selectively mark specific neuronal populations (e.g. Nathanson et al., 2009) which may be helpful one day in identifying cell type specific connections. In particular, transneuronal tracers relying on neurotrophic viruses that are able to traverse multisynaptic pathways are used to directly reveal neural circuits. Recent improvements based on genetic modifications provide an enhanced control over their selectivity and their viral spread (Callaway, 2008).

In Tables 3 and 4 we list a number of studies providing data on the morphology of individual axons, including long-range axon collaterals. Table 3 contains studies relying on intracellular injections. Table 4 refers to studies based on extracellular injections, but where the authors were able to follow single axons leaving the injection site. All these studies reported patchy distant projections also for individual PCs. These studies also indicate that an individual PC may contribute to several patches. As before, we listed the patch parameters inferred from these studies and, additionally, the layer of the injection site. Most of these studies considered only intrinsic projections; axons descending into the white matter were not followed further. In contrast, Table 1

Table 2
List of publications on patchy projections resulting from extracellular injections focusing on retrogradely labeled cells, same order and nomenclature as for Table 1.

Literature	Species	Cortical areas	σ	N_p	θ_p	d_p	$d_{pmax}(\Sigma)$	d_{cc}
Huntley and Jones (1991)	macaque	motor cortex (intr.)	0.6–0.8		0.7–0.9, smaller for large d_p		8	0.3–0.5, 1 for large d_p
Kritzer and Goldman-Rakic (1995)	macaque	PFC (intr.)	0.1–0.5		0.2–0.8		5–7	0.5–0.8
Livingstone and Hubel (1984)	macaque	V1 (intr.)	≤ 0.15		0.1–0.2		1	
Gilbert and Wiesel (1989)	cat	V1,2	≤ 0.2		0.25–0.8	0.5–4	(6–8)	
Matsubara et al. (1987)	cat	V2 (intr.)		2–10	0.35	1.4	3.4	1
Read et al. (2001)	cat	A1 (intr.)			0.8×0.7	1.5, 3.2, 2.4	3.5	

Table 3

List of publications on 2D or 3D reconstructions of single patchy PC projections, ordered according to the species brain size and the cortical area they refer to. Listed are the layers, the average number of patches per cell/axon N_p , the average patch diameter θ_p , the average and maximum lateral distance between the cell body and its patches d_p , $d_{p,max}$, the maximum lateral axonal spread Σ , and the average distance between the patches d_{cc} . All measurements are given in millimeters. Part one: intracellular injections.

Literature	Species	Cortical areas	Layer	N_p	θ_p	d_p	$d_{p,max}(\Sigma)$	d_{cc}
McGuire et al. (1991)	macaque	V1 (intr.)	3	4			2	0.4
Gilbert and Wiesel (1983)	cat	visual (intr.)	2–6		0.2–0.3	2	4	1
Martin and Whitteridge (1984)	cat	V1 (intr.)	2–5		0.1	0.2–2.2		1
Kisvárdy et al. (1986)	cat	V1 (intr.)	3		0.3–0.4	0.5–1	2	
Gabbott et al. (1987)	cat	V1	5/6	3		1.1–2.6		
Binzegger et al. (2007)	cat	V1	2–6	0–5	0.35–0.6	0.1–1.5	2.1	
Ghosh et al. (1988)	cat	4 γ (intr.)	2/3, 5	3–8			1.5	
Ojima et al. (1991)	cat	A1 (intr.)	2/3	2–4		0.5–2.5		
Lohmann and Rörig (1994)	rat	V2 (intr.)	2/3		0.18		1.2	0.2

Table 4

List of publications on 2D or 3D reconstructions of single patchy PC projections, continuation of Table 3. Part two: extracellular injections with single axon reconstructions.

Literature	Species	Cortical areas	Layer	N_p	θ_p	d_p	$d_{p,max}(\Sigma)$	d_{cc}
DeFelipe et al. (1986)	macaque	SI, motor cortex	WM	1–5			6	
Rockland and Virga (1989)	macaque	V2 to V1		1–3	0.3–0.5	0.6–4.3		0.36–0.65
Rockland and Virga (1990)	macaque	V1 to V2		1–3	0.2–0.35			0.2–0.5
Rockland (1995)	macaque	V2 to V5		1–3	0.2–0.4			0.2–0.6
Rockland and Knutson, 2001	macaque	V1 (intr.)	6		0.1		8	
Tyler et al. (1998)	macaque, marsupial	V1 (intr.)	2/3		0.32, 0.23			0.55, 0.4
Kisvárdy and Eysel (1992)	cat	V1 (intr.)	3	4–8	0.4	0.5–2.8	2.8 (4.9)	1.1
Clarke et al. (1993)	cat	A1					2–7	
Wallace and Bajwa (1991)	ferret	A1	2/3	6	0.3–0.8	1–4		

contains references to several studies that do include white matter projections (e.g. Pucak et al., 1996; Burkhalter and Bernado, 1989; Burkhalter and Charles, 1990; Melchitzky et al., 1998; Gilbert and Wiesel, 1989).

3.2.4. Quantitative data on patches

In this section, we discuss and substantiate in more detail the patch parameters we chose for the model outlined in Section 2. Tables 1–4 summarize the results of a large number of studies on patchy connections and provide estimates of the patch parameters N_p , θ_p , d_p , $d_{p,max}$, and d_{cc} , see Fig. 3. Depending on the experimental methods used (intra- or extracellular injections, see Section 3.2.3), we also listed the layer in which the cell body was localized or the size of the injection σ . Please note that the observations discussed in this section pertain to all areas and all species considered in Tables 1–4. Thus, the corresponding values are generalized averages. In particular, we neglected all outliers listed in Tables 1–4. In Section 4 we discuss the consequences of this procedure, and suggest some modifications for an adaption to specific areas.

3.2.4.1. Size of the patches. For the single cell/axon reconstructions (Tables 3 and 4), the measured patch diameters ranged from 0.1 to

0.8 mm, mostly, however, ranging from 0.2 to 0.4 mm. These values are similar to the data obtained from extracellular injections (Table 1). Here, θ_p ranged from 0.1 to 1 mm, but most reported values lie between 0.2 and 0.5 mm. Thus, group patches were only slightly larger than patches established by a single axon. This was already mentioned in Malach et al. (1994, squirrel monkey V2). The variations with respect to cortical areas or species was in most instances as large as the variations between different studies on one particular area in one particular species.

3.2.4.2. Lateral distance from a patch to the cell body. For the single-cell data d_p ranged from 0.4 to 6 mm, mostly confined to 1 or 2.5 mm. The maximum distance d_p lies between 1 and 7 mm, with most values between 2 and 4 mm. Again, the group data (Table 1) only slightly deviated from this: Here, d_p ranged from 1 to 8 mm, mostly confined between 1 and 3.5 mm, while d_p ranged from 2 to 8 mm, i.e. the lateral distances of the extracellular injection data were slightly larger. The largest values occur for monkey PFC. Similarly, higher visual areas (TE, TEO), motor and somatosensory areas in the macaque monkey exhibit comparably large d_p . Due to a lack of data these values cannot be compared to other species.

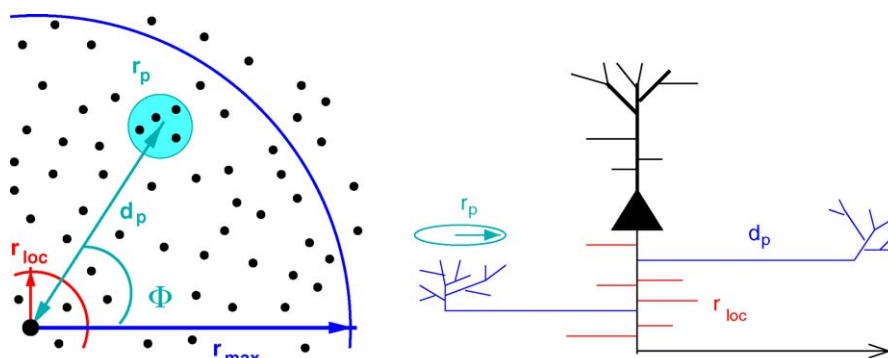


Fig. 3. Parameters of patchy projections. Left: Detail from Fig. 1 describing the size of a patch r_p , and its position relative to the cell body, described by d_p and Φ . Top view on the flattened cortex. Right: Lateral view of the cortex with a single schematic pyramidal cell forming two patches.

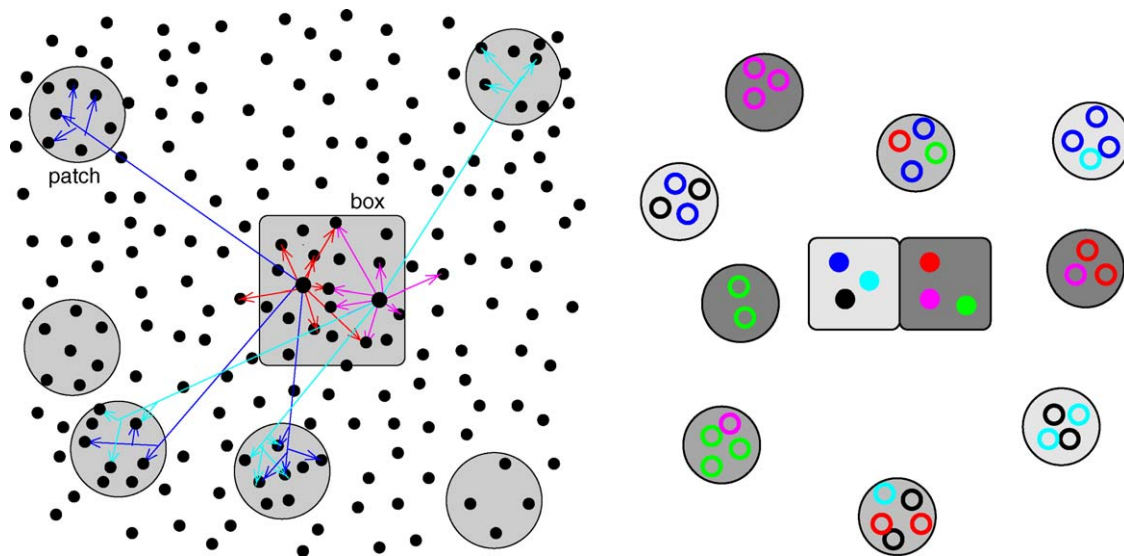


Fig. 4. Scheme illustrating the patchy projection pattern (disks) of a group of adjacent neurons (represented by dots in a quadratic box), matched to data from extracellular tracer injections. Left: Example of two cells located in a box that form local (red, magenta) and patchy distant projections (blue, cyan), sharing two of their terminal fields. Right: Simplified scheme of the joint projection pattern: two sets of 3 single cells (filled colored dots) located within two neighboring boxes (squares), each of them projecting to 3 out of 6 common patches (disks). The color of each synapse (small open circle) indicates the cell by which it is established.

3.2.4.3. Number of patches. The number of patches N_p reported for single cells/axons was between 1 and 8, rarely exceeding 6, with an approximate average value of 3.5 patches per neuron. However, the number of patches N_p resulting from extracellular injections ranged from 2 to 58, mostly confined between 10 and 20. Yet, this parameter depends significantly on the injection size, see below.

As analyzed by Amir et al. (1993, macaque V1, V2, V4, 7a) and Malach et al. (1997, owl monkey V5) a larger injection led to more patches, whereas their size hardly increased. Thus, the total cortical area targeted by lateral connections was enlarged. For example, increasing σ from 0.15 to 0.35 mm led to a 6-fold increase in the total patch area, see Malach et al. (1997). In agreement with this, Yoshioka et al. (1992, macaque V4) reported that even for injections smaller than ϕ_p the patch size and interval are nearly equivalent to those found for larger injections, but N_p and the spatial spread are smaller. In addition, Rumberger et al. (2001, rat V1,2) reported that doubling the injection size did not lead to a twofold ϕ_p . Likewise, Tanigawa et al. (2005, macaque V1, TE) found that a larger σ resulted in a more widespread distribution. However, they reported the development of large band-like patches near the injection site in V1, probably due to a fusion of single patches near the injection site, see also Levitt et al. (1994, macaque V2). Likewise, Lund et al. (1993, macaque) found some tendency for merging patches in V2 and PFC, as well as for an elongation of patches in motor and somatosensory cortex. Yet, despite this tendency, the spatially clustered projection patterns persist for large injections, with a fixed upper limit in patch size or width, and no filling in of gaps distant from the injection site. In particular, the large injections of HRP (horseradish peroxidase) into V1 ($\sigma = 0.5$ up to 1.5 mm) in Rockland et al. (1982, tree shrew) and Rockland and Lund (1983, squirrel and macaque monkeys) reveal a smooth transition between the homogeneously labeled local halo surrounding the injection site to distant discrete patches: the rim region of the local halo is disrupted by label-free zones, while beyond this distance, the HRP label appears as regularly spaced discrete patches.

3.2.5. Overlapping patches of adjacent neurons

The relation between injection size and number and size of individual patches helps to address two important questions: (1) To what degree do axon terminals of different neurons from the same injection site target identical (or at least overlapping) regions

as indicated in Fig. 4? (2) If they do so, does the amount of overlap in their terminal fields depend on the distance between the cells at the injection site? If there was a partial overlap, and if its size depended on the distance between the source neurons, an increase in injection size would induce a corresponding increase in patch size. As discussed before, this does not seem to be the case. Moreover, one would expect a tendency for distant patches to fuse, or a filling-in of the gaps between the stained regions, which is not the case either (Lund et al., 1993; Malach et al., 1993). The assumption that a systematic shift in the location of the source neuron would give rise to a corresponding systematic shift in its ramifications would, for a larger group of source neurons (represented by the box in Fig. 4), result in a more or less homogeneous arrangement of fiber terminals and not in clustered terminal fields (disks in Fig. 4). Thus, the answer to question (2) is a clear “no”, as patches resulting from extracellular injections are well-established. As long as the neurons are located within a certain maximum range, their distance to each other does not seem to affect the relative patch positions and sizes.

Likewise, in the case of randomly distributed single-cell terminal fields from one injection site, extracellular tracer injections would lead to a homogeneous projection pattern. Let us assume that all neurons in a sheet of cortex are arranged in distinct groups of adjacent neurons, and that each group establishes an individual pattern of patchy projections. Then, increasing the injection size in such a way that it reaches more initial groups would result in significantly more, widely distributed patches without affecting the patch size – similar to the findings in Amir et al. (1993) and Malach et al. (1997), see previous Section. Thus, the answer to question (1) is: some – but not all – cells in a certain neighborhood share some – but not all – of their terminal fields. Moreover, retrogradely stained patches directly indicate that adjacent neurons receive synapses from several distant groups, contradictory to the assumption that all synapses in a patch originate from adjacent neurons. In particular, the co-registration of clustered projection patterns resulting from both anterograde and retrograde transport is strongly indicative of reciprocal connections (Luhmann et al., 1986, cat area 17; Kisvárdy and Eysel, 1992, cat area 17; Levitt et al., 1994, macaque V2, Pucak et al., 1996; Yousef et al., 1999, cat area 18, Angelucci et al., 2002a,b, macaque V1).

Johnson et al. (2000) stated that the projections of intracellularly filled adjacent PCs in the piriform cortex of the rat showed little overlap. Gabbott et al. (1987) reported that the patchy projections from V1 to V2 of two intracellularly filled Meynert cells in the monkey cortex, separated by 0.9 mm, partly overlapped. The study by Kisvárdy and Eysel (1992, cat area 17) was based on extracellular injections, but they were able to reconstruct the axonal and dendritic arborization of 10 individual PCs. They found coinciding axon terminals, but not necessarily from direct neighbors. The superposition of these 10 PCs revealed a patchy network, with each PC sharing 2–5 of its patches (including the local one) with the patches of other PCs. Ojima and Takayanagi (2004, cat A1) reported that the amount of overlap in axonal terminal fields of two extracellular injections depended both on the spatial distance between the injection sites and on the distance from patch to injection site: axon terminals located more distally from the injection site frequently coincided if the injection sites were separated by less than 1 mm. In monkey TE the results of adjacent tracer injections (0.54 and 0.62 mm center-to-center distance) indicate that sets of terminal patches emanating from adjacent cortical sites are primarily independent (Tanigawa et al., 2005). The axis of the corresponding anisotropic patch distributions varied and there was only very little overlap.

The investigation of overlapping projection patterns imposes challenging experimental demands since it requires a successful and complete staining of two neurons or neuronal populations, without mutual interference (see Section 3.2.3). These difficulties could lead to an underestimation of such an overlap, in particular for the most distant fiber terminals, and for injection sites located more than 1 mm apart. In summary, pyramidal cells located around 1 mm apart (or even more, see above) may share some of their distant patch(es), while directly neighboring cells do not always do so.

In general, the occurrence of common pre- or postsynaptic neurons depends presumably not only on the distance between any two neurons (or any two groups of adjacent neurons). As mentioned in Section 3.2.2, the functional properties of these neurons may also play an important role in determining such overlapping connectivity patterns (e.g. Matsubara et al., 1987). Naturally, a statistical model based on a merely distance dependent connectivity cannot account for such functional aspects - unless one assumes an underlying functional architecture (e.g. orientation maps) and additional rules for the connection probability (e.g. preferred 'like to like' connections).

4. Validity and specifications of the generalized model

So far we may conclude that, in a global, statistical sense, it is justified to assume our model of patchy long-range projections to be the general case. Nonetheless, it is important to compare the projection pattern in different areas and/or species, and to pay attention to the exceptions. For example, in the rat piriform cortex, connections were found not to be patchy, but projections outside this area again appeared to be clustered (Johnson et al., 2000). According to Van Hooser et al. (2006) the horizontal connectivity in the primary visual cortex of mammals without orientation maps could be another exception, a finding that will be discussed in Section 4.2.

Hence, on the one hand there are outliers our model does not account for. On the other hand, there are special cases that necessitate major or minor modifications of our model. For example, the pattern of horizontal connectivity in monkey PFC is such a special case. Here, the clustered projections are elongated, forming stripes rather than circular patches (Levitt et al., 1993; Lund et al., 1993; Pucak et al., 1996; Kritzer and Goldman-Rakic, 1995). Moreover, the distances from a given injection site to the most distant stripes are comparably large (see Table 1). This leads

to an enlargement of the parameter d_p , in addition to a minor modification of our model, the departure from our isotropic connectivity assumption in order to incorporate stripes. One has to define a preferred stripe direction, to introduce a stripe length while the parameter that originally described the patch diameter \varnothing_p can be applied to the stripe width (Lund et al., 1993).

Similar changes are necessary to adapt the generalized model to motor or somatosensory areas in macaque monkey. Based on the studies of Huntley and Jones (1991), Juliano et al. (1990), and Lund et al. (1993) we suggest to increase d_p and \varnothing_p , and to assume patches that are less well defined than, for instance, in visual cortical areas. To this end, one needs to incorporate synapses in between the patches (see also Section 5.1). Concerning single cell axons this means a less target-oriented but more diffuse fiber terminal distribution that shows nonetheless spatially clustered boutons (see also Defelipe et al., 1986).

Generally, a detailed comparison between different areas in one species or, in turn, a comparison of the connectivity patterns between different species in one area is difficult because most data concerns the visual areas of cats and macaque monkeys, see Tables 1–4. Therefore, our generalized model with the parameters suggested in Section 2 is mainly representative for V1 and V2 in macaque monkeys and cats (areas 17, 18). However, in this case a prominent feature of the spatial layout is missing, the anisotropy of the axonal fields: anterogradely labeled axons extend for longer distances and give off more terminal boutons (patches) along one axis compared to the orthogonal one. In the visual cortex of macaques several studies observed an anisotropy ratio in the range of 1.56 to 2.1 (Yoshioka et al., 1996, V1; Malach et al., 1993, V1; Angelucci et al., 2002a, V1; Tanigawa et al., 2005, V1 & TE; Fujita and Fujita, 1996, TE & TEO; Levitt et al., 1994, V2). This feature has also been reported for squirrel and owl (i.e., new world) monkeys (Sincich and Blasdel, 2001, V1; Malach et al., 1994, V2) and for the primary visual cortex of tree shrews (Bosking et al., 1997, Mooser et al., 2004). Similarly, Gilbert and Wiesel (1983), Luhmann et al. (1986) and Kisvárdy and Eysel (1992) observed an anisotropic spatial spread of single axons in cat area 17, although Buzás et al. (2006) state that an isotropic 2D Gaussian distribution fits best when modeling the spatial distribution of boutons at the population level in the cat.

Hence, in order to truly represent monkey or tree shrew V1 our model requires a minor change: the introduction of a preferred projection direction, leading to an anisotropic spatial arrangement of the patches. Concerning the anisotropic distribution of patches, similar findings have been reported for cat A1 (Clarke et al., 1993; Ojima et al., 1991; Ojima and Takayanagi, 2004). In general, the single cell projections described for cat A1 are similar to that in V1 (Ojima et al., 1991; Clarke et al., 1993).

Thus, differences exist in the details of the spatial connectivity profiles with respect to the functional focus of cortical areas. The following section describes possible rules characterizing the differences in the lateral projection pattern with regard to cortical hierarchy. Then, in Section 4.2, we attempt to compare the projection pattern of different species, mainly using the example of V1.

4.1. Cortical hierarchy and patches

There is a trend for an increase in the complexity of the structure of PCs from V1 to V2 to higher visual areas of the macaque monkey, i.e. an increase in the size of dendritic trees and receptive fields, coupled with more dendritic branches and a higher density of spines (Elston, 2007). A similar trend is valid for the somatosensory areas 3b, 5 and 7, and also from the motor to the premotor cortex. This trend is correlated with a similar one in the diameter of intrinsic axonal patches: Lund et al. (1993) found that

the size of intrinsic axonal patches is closely scaled to the size of the basal dendritic fields of layer 2/3 PCs in visual, somatosensory and motor areas in the macaque. And indeed, an increase in the average diameter of the patches from V1 to V4 to 7a could be found (Amir et al., 1993).

This increase in patch size is, however, small (a factor of about 1.3) compared to other measures: Amir et al. (1993) found a more impressive increase with respect to the average interpatch distance (our d_{cc} ; factor of 2.6), the average distance of the patches from the center of the injection site (our d_p ; factor of 3.4), and, in particular, the maximum range between the two most extreme patches (corresponding to our Σ ; factor of 4.2). This finding was even more pronounced when normalizing with the size of the area: in this case the total axonal spread of intrinsic patches was 13 times larger in 7a than in V1. There was also an increase in the number of patches from V1 to V4.

Findings by Yoshioka et al. (1992) point in the same direction: they also found slightly larger patches in V4 as compared to V1 and V2 (from 200–300 in V1 up to 250–450 μm in V4) and a greater patch spacing in V4 (about 600 μm in average) as compared to V1/V2 (an average between 400 and 500 μm).

The trend in the increase in patch size and, in particular, in the larger spatial spread of patches when moving away from the primary visual cortex is confirmed by studies on the temporal cortex: Fujita and Fujita (1996) compared patch sizes in TEO and TE of the macaque to that in V1, V2 and V4 in the studies mentioned above: The diameter of the patches in TEO and TE was larger than that in the hierarchically lower visual areas. This is corroborated in a study by Tanigawa et al. (2005) who directly compared the organization of intrinsic horizontal connections in V1 and TE of the macaque. They clearly confirm a larger patch size, and in particular also a larger interpatch distance (d_{cc}) and larger spatial spread from the injection site (d_p).

Concerning areas 17 and 18 in the cat visual cortex Kisvárdy et al. (1997) did not find a discernible difference in average patch size while the average distance between patches was larger in area 18.

4.2. Model validity with respect to different species

Due to our modeler's perspective we expected that several aspects of the patchy projection pattern scale with brain size or volume. Basically, we reckoned the patch size \emptyset_p , the spatial range d_p , as well as the inter-patch distance d_{cc} to increase from, for instance, tree shrew to cat to macaque cortex. However, this is not what we found in the literature. In contrast, comparing the values for \emptyset_p , d_p , d_{cc} , Σ , and d_{cc} in Tables 1–4 for one area, e.g. V1, of different species we stated that they are astonishingly similar. The variations between different studies in one species are as large as the variations between different species. There are also some studies that directly investigate this issue. For example, Tyler et al. (1998) analyzed the intrinsic organization of V1 of three types of mammals, the macaque and two marsupials (the dunnart and the quokka), and compared their findings to V1 of rats and cats (area 17). The surface area of V1 in the macaque is circa 3 times larger than in cats, 13 times larger than in quokka, and approximately 200 times larger than in the rat or dunnart. Nevertheless, in case they found patchy connections (not in dunnarts and rats), \emptyset_p ranges from 228 (macaque) to 318 μm (quokka), and d_{cc} from 400 (macaque) to 600 μm (cat). In addition, Bugbee and Goldman-Rakic (1983) compared the size and the pattern of cortico-cortical projections in the PFC of squirrel and macaque monkeys. The neocortical volume of the macaque is approximately 4.5 times larger than that of a squirrel monkey but the width of cortical columns are relatively similar: 685 μm for the macaque versus 555 μm in the squirrel monkey. Thus, considering these findings, we cannot provide any scaling relations for the parameters of our model with respect to different species.

Still, there is the special case of horizontal connectivity in the visual cortex of mammals without orientation maps. In this case, patchiness is less obvious. Van Hooser et al. (2006) even stated that the long-range intrinsic connections in the primary visual cortex of the gray squirrel, a rodent without orientation maps, are not patchy but show a distinct spatial organization compared to other mammals. At first glance, this seems to contradict the findings of other studies (Lohmann and Rörig, 1994, using single neuron reconstructions; Rumberger et al., 2001; Kaas et al., 1989; Burkhalter, 1989; Burkhalter and Charles, 1990; all using antero- and/or retrograde tracing in V1 and/or V2) that report – some – clustered projection patterns, similar to those in cat and macaque visual cortex. Van Hooser et al. (2006), however, did not account for single cell projections, instead they used only extracellular, retrograde tracing, and the study was strictly confined to intra-area connections. Burkhalter and Charles (1990) stated that the clustered projections in rat visual cortex can only be shown with small injections of anterograde tracer labeling. Given all these details, the inconsistency is alleviated. As stated in Section 3.2.1, in such small cortices intrinsic projections do not necessarily follow the same distance dependent rules as in larger ones, unless the existence of functional maps demands a specific connective organization, such as in V1 of tree shrews (Rockland et al., 1982; Bosking et al., 1997). Nevertheless, there are marked commonalities in the patchy connection patterns of rats and other species (Rumberger et al., 2001; Malach, 1989), in particular if one does not strictly separate between V1 and V2. In terms of modeling rat visual cortex, we suggest to consider a combination of V1 and the surrounding rim region.

5. Discussion

Section 2 presented our cortical network model: a 2D spatially embedded network of neurons with local ($r_{loc} = 0.5$ mm) and distant ($r_{max} = 4$ mm) connections, the latter established in patches ($N_p = 3$, $\emptyset_p = 0.5$ mm). In Section 3 we reviewed the corresponding neuroanatomical data, and in Section 4 we already discussed the aspect of generalization.

Comparing the patchy projection patterns of different areas and different species, we suggested several adaptations of the model. We found more and larger differences with respect to distinct areas than in one area of different species. In our view, the functional requirements of a certain region are the most important factors that determine its connectivity. These are obviously given in terms of their input modalities and the cortical processing system they belong to, e.g. visual, auditory, prefrontal or somatosensory cortex. Yet, functional specifications also exist in terms of the hierarchical level in cortical processing, e.g. orientation selectivity in V1, and object recognition in the inferior temporal cortex (area TE: Fujita and Fujita, 1996; Tanigawa et al., 2005).

We will now compare the *general* features of our model and its parameters to experimentally established cortical reality, and propose possible directions for future research. In this context, and with regard to the modeler's perspective, it is worth mentioning that the published data on long-range patchy connections is not restricted to purely structural properties. Further information on more functional parameters like the shapes of excitatory postsynaptic potentials, and the corresponding conduction velocity is available, e.g. (Bringuier et al., 1999; Yoshimura et al., 2000, both cat area 17; Lohmann and Rörig, 1994, rat V1).

5.1. Basic spatial settings and local connections

Our choice of network model size (square sheet of cortex with side length $R = 8$ mm) appears to be well substantiated: in most studies on single cell data, patches and cell body are maximally

$d_p \sim 2 - 4$ mm apart, in the group data $d_p \sim 2 - 8$ mm. Since we aim to design a generalized model, our restriction of $r_{\max} = d_p = 4$ mm is, therefore, reasonable. Moreover, our distance dependent connectivity scheme (cf. Fig. 2) largely matches what is described in the literature. We have shown several examples confirming that the separate treatment of local and distant intrinsic connectivity is justified. These two systems exhibit different characteristics, in particular concerning their spatial settings and their functional aspects.

In our model, the local connectivity is restricted by the space constant r_{loc} (Section 2). We chose a large value for this local connectivity range $r_{\text{loc}} = 0.5$ mm, the maximum value we found in the literature (Section 3.1), to compensate for having selected a low density of neurons (imposed by computational constraints; see also below). In our model, local connections are established according to a circular but flat probability profile. This choice of using a constant p_{loc} for all neurons located within $r < r_{\text{loc}}$ is a clear simplification, as in the cortex the probability for a local synapse decays monotonically with distance.

We assigned a certain percentage of the presynaptic sites of each neuron to be local. In Section 3.2.1 we explained why we assume the remainder, the intrinsic distant connections, to exhibit patchy projections. These two aspects lead to a critical point concerning our choice of model parameters: In most cases, we fixed a specific value for each parameter, instead of admitting a distribution of values. Thus, rather than assigning every single PC the same percentage of local axonal connections (60%), it would be more realistic to use a distribution of values, e.g., 40–75%, from which a value is drawn for each cell. Likewise, we simplified by assuming that all distant connections are patchy (Section 3.2), although this is not in full agreement with the – sparse – literature on this topic. At any rate, not all distant synapses are arranged in spatial clusters, individual axons can establish synaptic boutons on their way to the patches (Amir et al., 1993; Yabuta and Callaway, 1998; Kisvárdy et al., 1997), in particular in the motor or somatosensory cortex (Section 4). Here, we neglected such ‘en passant’ synapses. The question is, how many of such synapses exist, and what are the implications of neglecting them. If the axon is myelinated, the possibility of ‘en passant’ synapses is limited to the nodes of Ranvier, i.e., presumably negligible. If the axon is not myelinated, though, the density of synapses along such an axon (at least in the macaque) can be as high as on its terminal ramifications (Amir et al., 1993). Both kinds of long-range collaterals exist: in a combined light and electron microscopic study of 2 pyramidal cells in the cat visual cortex, Kisvárdy et al. (1986) found the horizontally traveling axon collaterals to be myelinated. In monkey, DeFelipe et al. (1986) distinguished between unmyelinated minor collaterals near the soma and myelinated major collaterals, which often show no branching within a distance of 0.8 mm. Ghosh et al. (1988) stated that ‘en passant’ boutons occur in the local range of 0.5 mm, but not on long-range collaterals. In Ojima et al. (1991) the observations were similar: at a distance larger than 0.7 mm there are less boutons ‘en passant’ than in the local range, whereas Clarke et al. (1993) observed both, axons with and axons without boutons on their way. In view of this variability in the anatomical data, we are currently not in a position to draw a final conclusion regarding the potential importance of such more distant ‘en passant’ synapses.

5.2. Patches and single-cell data

In our model, the remote synapses of a neuron are uniformly distributed among its three patches (cf. Fig. 4, right). Here, it would also be reasonable to incorporate some variability. For example, the number of synapses in a patch could depend on its distance to the cell body: Kisvárdy and Eysel (1992, cat area 17) and Malach

et al. (1994, squirrel monkey V2) observed a lower bouton density in distant patches. Likewise, Tanigawa et al. (2005, macaque) show a strong (V1) or moderate (TE) decrease in labeling intensity of patches with increasing distance to the injection site, and Wallace et al. (1991, cat A1) reported small distant patches with less labelled fibers. Otherwise, the number of synapses in a patch could depend on its size, e.g. Rockland and Virga (1989, 1990, macaque V1,2) reported that large clusters showed a lower bouton density. In particular, Binzegger et al. (2007) analyzed the relation between the number of patches, their sizes, and the associated bouton densities. In brief, they ranked the single-cell patches according to their bouton densities, and found that – apart from the rank 1 patch (highest bouton density, typically above or around the location of the cell body) – boutons were indeed approximately uniformly distributed among patches. The number of patches N_p tended to determine their size and bouton density, but both N_p and the total number of boutons varied considerably across neurons. Thus, cortical connectivity is remarkably heterogeneous, with several studies discussed here revealing large variations within their own results (Kisvárdy et al., 1997; Buzás et al., 2006). The latter study strongly emphasizes the single cell variability compared to the population level. Therefore, a future model should be extended to take this variability into account.

Generally, our patch parameters N_p , \emptyset_p and d_p match the values given by the literature quite well. The number of patches $N_p = 3$ agrees with the documented values for the number of single cell patches. However, instead of assuming the same value of this parameter for all neurons, it would be more adequate to draw the individual values from a suitable distribution. For the patch size we selected a diameter of 0.5 mm. This matches the restricted range of values for the group patches $\emptyset_p \sim 0.2-0.5$ mm, but is slightly beyond the restricted range for single cell patches $\emptyset_p \sim 0.2-0.4$ mm. For reasons discussed below we nevertheless chose the somewhat larger diameter. Once more, it would be more realistic to include a variable patch size. For the distance between the cell body and the patch center we drew values between 0.75 and 3.75 mm from a uniform distribution. One could, however, also postulate a distance dependent probability of the patch position, e.g., a Gaussian profile. Several studies on the visual cortex of cats and macaques report a decreasing number of patches with increasing distance from the injection site or cell body, respectively (Levitt et al., 1994; Tanigawa et al., 2005; Binzegger et al., 2007). Similarly, Buzás et al. (2006, cat area 17) and Bosking et al. (1997, ferret V1) found a distant dependent decay in the number of boutons for both, the local and long-range connectivity.

5.3. Patches and group data

A comparison of our grouping assumptions with the literature (Table 1) is difficult because – due to computational limitations – it is impossible to use a realistic neuronal density in our model. In Section 2 we compared the density of neurons in our model to that in the mouse cortex. In Section 4, however, we ascertained that our model rather represents cat area 17. We now compare to layer 2/3 of cat area 17: according to Beaulieu and Colonnier (1989) the corresponding density is approximately 22 100 PCs/mm² (binocular part, 0.464 mm thickness). Given $N = 100,000$ our model yields a density of 1562 PCs/mm², i.e. more than one order of magnitude too small. While an extension to a biologically realistic, much larger network size is conceptionally straightforward, numerical simulations impose challenging computational demands (Morrison et al., 2005). Hence, to compensate, we adapted some of our parameters, first, by assuming a rather large local connectivity range as explained above and, second, by somewhat overestimating the spatial extent of the group of neurons stained in extracellular tracer injections, explained as follows. To account

for the projection patterns of groups of neurons – as opposed to single-cell data – we considered groups of adjacent neurons located in boxes of side length $bl = 0.5$ mm. In Table 1 the corresponding measure is the injection size σ , which in most publications was in the range of 0.2 up to 0.4 mm, excluding the studies analyzing explicitly the effect of larger injections. Thus, our boxes are somewhat larger ($bl > \sigma$) than the typical injection size, in order to compensate for the low neuron density.

In reality, up to a few thousand neurons may have taken up the tracer at injection sites with a diameter of 0.2–0.4 mm (Schüz et al., 2005, for an estimate on the mouse cortex, using biotinylated dextran amine), though this number may depend on the tracer used and on brain size: considerably lower values have been reported for the cat cortex (Kisvárdy et al., 1997, using biocytin). The number of patches resulting from such extracellular injections in large brains is approximately $N_p = 10 - 20$. We assumed six patches per box corresponding to six patches for an extracellular injection of size bl , a bit larger than the measured size σ . This deviation is explained as follows: The critical point of the grouping assumptions (Fig. 4) is the overlap in the terminal fields of single neurons. Due to the difficulties in modeling a realistic neuron density, the number of neurons per box is underestimated. Thus, it would be inappropriate to distribute their synapses to more than six patches, as this would further reduce the probability of neurons within a box targeting identical postsynaptic cells. In addition to the grouping assumptions (Fig. 4, left), one could increase the probability for shared terminal fields by adopting the following additional rule: Instead of considering one box at a time, we could consider pairs of adjacent boxes such that, when moving from one box to the next, some number (e.g., four out of six) projection patches are shared, rather than changing all six patch positions (Fig. 4, right, see also Voges et al., 2010). This leads to shared terminal fields even for neurons located at a distance of more than $bl = 0.5$ mm apart, see Section 3.2.5.

5.4. What we did not include

We did not consider target selectivity, thus we will not discuss the long standing controversy of randomness versus specificity in cortical connectivity (e.g. Yoshimura and Callaway, 2005; and the special issue of the Journal of Neurocytology Vol. 31, no. 3–5, 2003). However, raising the question whether patchy pyramidal cell (PC) connections are reciprocal brings us close to this issue. For example, Morishima and Kawaguchi (2006) showed that sub-populations of corticostriatal neurons in the rat frontal cortex are selectively connected to each other. Kisvárdy et al. (1986) and Kisvárdy and Eysel (1992) found that a pyramidal cell located within the axonal patch of another distant pyramidal cell in cat area 17 often sent, in turn, an axonal patch back to the dendritic tree of this distant pyramidal cell. Hence, they suggested a specific network of reciprocal patchy PC connections. Likewise, Lewis et al. (2002) proposed the neuroanatomical substrate for a specific network of feedforward excitation and local feedback inhibition, based on their findings that only about 50% of the local targets of PCs were other PCs, while PCs constituted more than 90% of the distant intrinsic and long-range projection targets (Melchitzky et al., 2001). These authors had also evidence for the existence of monosynaptic reciprocal connections (Melchitzky et al., 1998). Moreover, it is assumed that patchy projections predominantly connect domains with similar functional properties (Section 3.2.2). Thus, there is indeed evidence for a certain amount of target selectivity in patchy PC projections, to what extent, however, remains a matter of debate.

As mentioned in Sections 2 and 3 we did not consider the vertical structure of the cortex, i.e., specific connections across cortical layers. Concerning local projections, the neuroanatomical

literature provides various studies on the intra- and interlaminar connectivity (e.g., Thomson and Bannister, 2003; Bannister, 2005; Douglas and Martin, 2004), but regarding long-range projections, less information is available. To model intra- and interlaminar connections, however, one has to know both the source and the target layers for each long-range axon collateral. In Tables 3 and 4, we listed the layers of the injection sites that gave rise to single axon reconstructions. Assuming a strictly lateral fiber course, source and target layer would be largely identical, and the patchy projections would predominantly occur in layers 2/3 and less often in layers 4 or 5.

Another issue, not included in the present model, concerns the white matter connections. In the macaque prefrontal cortex, Lewis et al. (2002) showed that these connections are very similar to the intrinsic ones, e.g., with respect to the number of patches and their spatial extent. Moreover, according to Gilbert and Wiesel (1989) and Burkhalter and Bernardo (1989), there is no significant difference in the projection schemes of white matter and grey matter connections: both can be patchy in a similar way. Finally, the economy argument of minimizing cable length by invoking patchy projections would seem even more important for the long cortico-cortical projections.

6. Conclusions

We suggest a general model of the horizontal cortical connectivity and matched its parameters to the published neuroanatomical data. In spite of the sparseness and high variability of these data, several key characteristics and quantities differed only slightly across cortical areas and animal species. Moreover, it is straightforward to adapt the model to specific properties of any particular area. The primary remaining problem is the neuronal density: If one intends to model an $8\text{ mm} \times 8\text{ mm}$ sheet of cortex, the number of neurons vastly exceeds current computational limits. However, it seems to be possible to adapt most of the relevant parameters in a reasonable way, without losing the key structural properties of interest.

Acknowledgements

We thank Valentino Braitenberg and Christian Guijarro for stimulating discussions. This work was funded by a dissertation grant to N.V. from the IGPP Freiburg. Further support was received from the German Federal Ministry of Education and Research (BMBF grant 01GQ0420 to BCCN Freiburg), from the Future and Emerging Technologies (FET) program within the Seventh Framework Program for Research of the European Commission, under the FET-Open grant agreement BION (number 213219), and from the German Research Foundation (CRC 780, subproject C4).

References

- Amir, Y., Harel, M., Malach, R., 1993. Cortical hierarchy reflected in the organization of intrinsic connections in macaque monkey visual cortex. *J. Comp. Neurol.* 334, 19–46.
- Amirikian, B., 2005. A phenomenological theory of spatially structured local synaptic connectivity. *PLOS Comput. Biol.* 1 (11), 74–85.
- Anderson, J.C., Martin, K.A.C., 2006. Synaptic connections from cortical area V4 to V2 in macaque monkey. *J. Comp. Neurol.* 495, 709–721.
- Angelucci, A., Levitt, J.B., Walton, E.J.S., Hupe, J.M., Bullier, J., Lund, J.S., 2002a. Circuits for local and global signal integration in primary visual cortex. *J. Neurosci.* 22 (19), 8633–8646.
- Angelucci, A., Levitt, J.B., Lund, J.S., 2002b. Anatomical origins of the classical receptive field and modulatory surround field of single neurons in macaque visual cortical area V1. *Prog. Brain Res.* 136, 373–388.
- Angelucci, A., Bullier, J., 2003. Reaching beyond the classical receptive field of V1 neurons: horizontal or feedback axons? *J. Physiol. Paris* 97 (2–3), 141–154.
- Angelucci, A., Bressloff, P.C., 2006. Contribution of feedforward, lateral and feedback connections to the classical receptive field center and extra-classical receptive field surround of primate V1 neurons. *Prog. Brain Res.* 154, 93–120.

- Bannister, A.P., 2005. Inter- and intra-laminar connections of pyramidal cells in the neocortex. *Neurosci. Res.* 53, 95–103.
- Bassett, D.S., Bullmore, E., 2006. Small-world brain networks. *Neuroscientist* 12 (6), 512–523.
- Beaulieu, C., Colonnier, M., 1989. Number of neurons in individual laminae of areas 3b, 4y, and 6a α of the cat cerebral cortex: a comparison with major visual areas. *J. Comp. Neurol.* 279, 228–234.
- Beaulieu, C., 1993. Numerical data on neocortical neurons in adult rat, with special reference to the GABA population. *Brain Res.* 609, 284–292.
- Binzegger, T., Douglas, R.J., Martin, K.A.C., 2004. A quantitative map of the circuit of cat primary visual cortex. *J. Neurosci.* 24 (24), 8441–8453.
- Binzegger, T., Douglas, R.J., Martin, K.A.C., 2007. Stereotypical bouton clustering of individual neurons in cat primary visual cortex. *J. Neurosci.* 27 (45), 12242–12254.
- Bosking, W.H., Zhang, Y., Schofield, B., Fitzpatrick, D., 1997. Orientation selectivity and the arrangement of horizontal connections in tree shrew striate cortex. *J. Neurosci.* 17 (6), 2112–2127.
- Braak, H., Braak, E., 1986. Ratio of pyramidal versus non-pyramidal cells in the human frontal isocortex and changes in ratio with ageing and Alzheimer's disease. In: Swaab, D.F., Fliers, E., Mirmiran, M., Van Gool, W.A., Van Haaren, F. (Eds.), *Progress in Brain Research*. Elsevier, Amsterdam, pp. 185–212.
- Braitenberg, V., 2001. Brain size and number of neurons: an exercise in synthetic neuroanatomy. *J. Comput. Neurosci.* 10 (1), 71–77.
- Braitenberg, V., Schüz, A., 1998. *Cortex: Statistics and Geometry of Neuronal Connectivity*, 2nd ed. Springer-Verlag, Berlin.
- Bringuier, V., Chavane, F., Glaeser, L., Fregnac, Y., 1999. Horizontal propagation of visual activity in the synaptic integration field of area 17 neurons. *Science* 238, 695–698.
- Brunel, N., 2000. Dynamics of sparsely connected networks of excitatory and inhibitory spiking neurons. *J. Comput. Neurosci.* 8 (3), 183–208.
- Budd, J.M.L., Kisvárdy, Z.F., 2001. Local lateral connectivity of inhibitory clutch cells in layer 4 of cat visual cortex (area 17). *Exp. Brain Res.* 140, 245–250.
- Bugbee, N.M., Goldman-Rakic, P.S., 1983. Columnar organization of corticocortical projections in Squirrel and Rhesus monkeys: similarity of column width in species differing in cortical volume. *J. Comp. Neurol.* 220, 355–364.
- Burkhalter, A., 1989. Intrinsic connections of rat primary visual cortex: laminar organization of axon projections. *J. Comp. Neurol.* 279, 171–186.
- Burkhalter, A., Bernardo, K.L., 1989. Organization of corticocortical connections in human visual cortex. *Proc. Natl. Acad. Sci. U.S.A.* 86, 1071–1075.
- Burkhalter, A., Charles, V., 1990. Organization of local axon collaterals of efferent projection neurons in the rat visual cortex. *J. Comp. Neurol.* 302, 920–934.
- Buzás, P., Eysel, U.T., Kisvárdy, Z.F., 1998. Functional topography of single cortical cells: an intracellular approach combined with optical imaging. *Brain Res. Protocols* 3, 199–208.
- Buzás, P., Kovács, K., Ferecskó, A.S., Budd, J.M.L., Eysel, U.T., Kisvárdy, Z.F., 2006. Model-based analysis of excitatory lateral connections in the visual cortex. *J. Comp. Neurol.* 499, 861–881.
- Buzsáki, G., Geisler, C., Henze, D., Wang, X.-J., 2004. Interneuron diversity series: Circuit complexity and axon wiring economy of cortical interneurons. *TINS* 27 (4), 186–193.
- Callaway, E.M., 2008. Transneuronal circuit tracing with neurotropic viruses. *Curr. Opin. Neurobiol.* 18 (6), 617–623.
- Chisum, H.J., Mooser, F., Fitzpatrick, D., 2003. Emergent properties of layer 2/3 neurons reflect the collinear arrangement of horizontal connections in tree shrew visual cortex. *J. Neurosci.* 23 (7), 2947–2960.
- Chklovskii, D.B., 2000. Optimal sizes of dendritic and axonal arbors in a topographic projection. *J. Neurophysiol.* 83, 2113–2119.
- Chklovskii, D.B., 2004. Synaptic connectivity and neuronal morphology: Two sides of the same coin. *Neuron* 43, 609–617.
- Chklovskii, D.B., Schikorski, T., Stevens, C.F., 2002. Wiring optimization in cortical circuits. *Neuron* 34, 341–347.
- Clarke, S., Ribaupierre, F.d., Rouiller, E.M., Ribaupierre, Y.d., 1993. Several neuronal and axonal types from long intrinsic connections in the cat primary auditory cortical field (AI). *Anat. Embryol.* 188, 117–138.
- DeFelipe, J., Conley, M., Jones, E.G., 1986. Long-range focal collateralization of axons arising from corticocortical cells in monkey sensory-motor cortex. *J. Neurosci.* 6 (12), 3749–3766.
- DeLosRios, P., Petermann, T., 2007. Existence, Cost and Robustness of Spatial Small-World Networks. *IJBC* 17 (7), 2331–2342.
- Douglas, R.J., Martin, K.A.C., 2004. Neuronal circuits of the neocortex. *Annu. Rev. Neurosci.* 27, 419–451.
- Elston, G.N., 2007. Specializations in pyramidal cell structure during primate evolution. In: Kaas, J.H., Preuss, T.M., (Eds.), *Evolution of Nervous Systems*. Elsevier, vol. 5. Oxford, Elsevier.
- Erdős, P., Rényi, A., 1959. On Random Graphs. I. *Publicationes Mathematicae* 6, 290–297.
- Fujita, I., Fujita, T., 1996. Intrinsic connections in the macaque inferior temporal cortex. *J. Comp. Neurol.* 368, 467–486.
- Gabbott, P., Somogyi, P., 1986. Quantitative distribution of GABA-immunoreactive neurons in the visual cortex (area 17) of the cat. *Exp. Brain Res.* 61, 323–331.
- Gabbott, P., Martin, K.A.C., Whitteridge, D., 1987. Connections between pyramidal neurons in layer 5 of cat visual cortex (area 17). *J. Comp. Neurol.* 259 (3), 364–381.
- Galuske, R.A.W., Schlote, W., Bratzke, H., Singer, W., 2000. Interhemispheric asymmetries of the modular structure in human temporal cortex. *Science* 289, 1946–1949.
- Ghosh, S., Fyffe, R.E.W., Porter, R., 1988. Morphology of neurons in area 4 gamma of the cat's cortex studied with intracellular injection of HRP. *J. Comp. Neurol.* 269, 290–312.
- Ghosh, S., Porter, R., 1988. Morphology of pyramidal neurons in monkey motor cortex and the synaptic actions of their intracortical axon collaterals. *J. Physiol. (Lond.)* 400, 593–615.
- Gilbert, C.D., Wiesel, T.N., 1983. Clustered intrinsic connections in cat visual cortex. *J. Neurosci.* 5, 1116–1133.
- Gilbert, C.D., Wiesel, T.N., 1989. Columnar specificity of intrinsic horizontal and corticocortical connections in cat visual cortex. *J. Neurosci.* 9 (7), 2432–2442.
- Gilbert, C.D., 1992. Horizontal integration and cortical dynamics. *Neuron* 9, 1–13.
- Hellwig, B., 2000. A quantitative analysis of the local connectivity between pyramidal neurons in layers 2/3 of the rat visual cortex. *Biol. Cybern.* 82, 111–121.
- Hilgetag, C.-C., Burns, G.A.P.C., O'Neil, M.A., Scannel, J.W., Young, M.P., 2000. Anatomical connectivity defines the organization of clusters of cortical areas in the macaque monkey and cat. *Philos. Trans. Roy. Soc. London* 355, 91–100.
- Holmgren, C., Harkany, T., Zilberter, Y., 2003. Pyramidal cell communication within local networks in layer 2/3 of rat neocortex. *J. Physiol.* 551.1, 139–153.
- Hornung, J.-P., De Tribolet, N., 1994. Distribution of GABA-containing neurons in human frontal cortex: a quantitative immunocytochemical study. *Anat. Embryol.* 189, 139–145.
- Huntley, G.W., Jones, E.G., 1991. Relationship of intrinsic connections to forelimb movement representations in monkey motor cortex: a correlative anatomic physiological study. *J. Neurophysiol.* 66 (2), 390–413.
- Johnson, D.M.G., Illig, K.R., Behan, M., Haberly, L.B., 2000. New features of connectivity in piriform cortex visualized by intracellular injection of pyramidal cells suggest that primary olfactory cortex functions like association cortex in other sensory systems. *J. Neurosci.* 20 (18), 6974–6982.
- Jones, E.G., Hendry, S.H.C., DeFelipe, J., Benson, D.L., 1994. GABA Neurons and their role in activity-dependent plasticity of adult primate visual cortex. In: Peters, A., Rockland, K.S. (Eds.), *Cerebral Cortex*, Vol. 10, Primary visual cortex in primates, pp. 61–140.
- Juliano, S.L., Friedman, D.P., Eslin, D.E., 1990. Corticocortical connections predict patches of stimulus-evoked metabolic activity in monkey somatosensory cortex. *J. Comp. Neurol.* 298 (1), 23–39.
- Kaas, J.H., Krubitzer, L.A., Johanson, K.L., 1989. Cortical connections of area 17 (V1) and 18 (V2) of squirrels. *J. Comp. Neurol.* 281, 426–446.
- Kaiser, M., Hilgetag, C.C., 2004a. Modelling the development of cortical systems networks. *Neurocomputing* 58–60, 297–302.
- Kaiser, M., Hilgetag, C.C., 2004b. Spatial growth of real-world networks. *Phys. Rev. E* 69, 036103.
- Kalisman, N., Silberberg, G., Markram, H., 2003. Deriving physical connectivity from neuronal morphology. *Biol. Cybern.* 88 (3), 210–218.
- Karbowski, J., 2003. How does connectivity between cortical areas depend on brain size? implications for efficient computation. *J. Comput. Neurosci.* 15, 347–356.
- Kisvárdy, Z., Martin, K., Freund, T., Maglóczky, Z., Whitteridge, D., Somogyi, P., 1986. Synaptic targets of HRP-filled layer III pyramidal cells in the cat striate cortex. *Exp. Brain Res.* 64, 541–552.
- Kisvárdy, Z.F., Cowey, A., Smith, A.D., Somogyi, P., 1989. Interlaminar and lateral excitatory amino acid connections in the striate cortex of monkey. *J. Neurosci.* 9 (2), 667–682.
- Kisvárdy, Z.F., Eysel, U.T., 1992. Cellular organization of reciprocal patchy networks in layer III of cat visual cortex (area 17). *Neuroscience* 46, 275–286.
- Kisvárdy, Z.F., Toth, E., Rausch, M., Eysel, U.T., 1997. Orientation-specific relationship between populations of excitatory and inhibitory lateral connections in the visual cortex of the cat. *Cereb. Cortex* 7, 605–618.
- Kremkow, J., Kumar, A., Rotter, S., Aertsen, A., 2007. Emergence of population synchrony in a layered network of the cat visual cortex. *Neurocomputing* 70, 2069–2073.
- Kritzer, M.F., Goldman-Rakic, P.S., 1995. Intrinsic circuit organization of the major layers and sublayers of the dorsolateral prefrontal cortex in the Rhesus monkey. *J. Comp. Neurol.* 359, 131–143.
- Krone, G., Mallot, H., Palm, G., Schüz, A., 1986. Spatiotemporal receptive fields: a dynamical model derived from cortical architectonics. *Proc. R. Soc. Lond. B* 226, 421–444.
- Kumar, A., Rotter, S., Aertsen, A., 2008b. Conditions for propagating synchronous spiking and asynchronous firing rates in a cortical network model. *J. Neurosci.* 28 (20), 5268–5280.
- Kumar, A., Schrader, S., Aertsen, A., Rotter, S., 2008a. The high-conductance state of cortical networks. *Neural Comput.* 20 (1), 1–43.
- Levitt, J., Lund, J., 2002. Intrinsic connections in mammalian cerebral cortex. In: Schüz, A., Miller, R. (Eds.), *Cortical Areas: Unity and Diversity*. Taylor and Francis, pp. 133–154.
- Levitt, J.B., Yoshioka, T., Lund, J.S., 1994. Intrinsic cortical connections in macaque visual area V2: Evidence for interaction between different functional streams. *J. Comp. Neurol.* 342, 555–570.
- Levitt, J.B., Lewis, D.A., Yoshioka, T., Lund, J.S., 1993. Topography of pyramidal neuron intrinsic connections in macaque monkey prefrontal cortex (areas 9 and 46). *J. Comp. Neurol.* 338, 338–360.
- Lewis, D., Melchitzky, D., Burgos, G.-G., 2002. Specificity in the functional architecture of primate prefrontal cortex. *J. Neurocytol.* 31, 265–276.
- Lichtman, J.W., Sanes, J.R., Livet, J., 2008. A technicolor approach to the connectome. *Nat. Rev. Neurosci.* 9 (6), 417–422.
- Livingstone, M.S., Hubel, D.H., 1984. Specificity of intrinsic connections in primate primary visual cortex. *J. Neurosci.* 4 (11), 2830–2835.

- Lohmann, H., Röbig, B., 1994. Long-range horizontal connections between supra-granular pyramidal cells in the extrastriate visual cortex of the rat. *J. Comp. Neurol.* 344, 543–558.
- Luhmann, H.J., Martinez, M.L., Singer, W., 1986. Development of horizontal intrinsic connections in cat striate cortex. *Exp. Brain Res.* 63, 443–448.
- Lund, J., Yoshioka, T., Levitt, J., 1993. Comparison of intrinsic connectivity in different areas of macaque monkey cerebral cortex. *Cereb. Cortex* 3 (2), 148–162.
- Lund, J.S., Angelucci, A., Bressloff, P.C., 2003. Anatomical substrates for functional columns in macaque monkey primary visual cortex. *Cereb. Cortex* 12, 15–24.
- Malach, R., 1989. Patterns of connections in rat visual cortex. *J. Neurosci.* 9 (11), 3741–3752.
- Malach, R., Amir, Y., Harel, M., Grinvald, A., 1993. Relationship between intrinsic connections and functional architecture revealed by optical imaging and in vivo targeted biocytin injections in primate striate cortex. *Proc. Natl. Acad. Sci. U.S.A.* 90, 10469–10473.
- Malach, R., Tootell, R.B., Malonek, D., 1994. Relationship between orientation domains, cytochrome oxidase stripes, and intrinsic horizontal connections in squirrel monkey area V2. *Cereb. Cortex* 4 (2), 151–165.
- Malach, R., Schirman, T.D., Harel, M., Tootell, R.B.H., Malonek, D., 1997. Organization of intrinsic connections in owl monkey area MT. *Cereb. Cortex* 7, 386–393.
- Martin, K.A.C., Whitteridge, D., 1984. Form, function, and intracortical projections of spiny neurons in the striate visual cortex of the cat. *J. Physiol. (Lond.)* 353, 463–504.
- Matsubara, J.A., Cynader, M.S., Swindale, N.V., 1987. Anatomical properties and physiological correlates of the intrinsic connections in cat area 18. *J. Neurosci.* 7, 1428–1446.
- Matsuda, W., Furuta, T., Nakamura, K.C., Hioki, H., Fujiyama, F., Arai, R., Kaneko, T., 2009. Single nigrostriatal dopaminergic neurons form widely spread and highly dense axonal arborizations in the neostriatum. *J. Neurosci.* 29 (2), 444–453.
- McGuire, B.A., Gilbert, C.D., Rivlin, P.K., Wiesel, T.N., 1991. Targets of horizontal connections in macaque primary visual cortex. *J. Comp. Neurol.* 305, 370–392.
- Mehring, C., Hehl, U., Kubo, M., Diesmann, M., Aertsen, A., 2003. Activity dynamics and propagation of synchronous spiking in locally connected random networks. *Biol. Cybern.* 88 (5), 395–408.
- Melchitzky, D.S., Gonzalez-Burgos, G., Barrionuevo, G., Lewis, D.A., 2001. Synaptic targets of the intrinsic axon collaterals of supragranular pyramidal neurons in monkey prefrontal cortex. *J. Comp. Neurol.* 430, 209–221.
- Melchitzky, D.S., Sesack, S.R., Pucak, M.L., Lewis, D.A., 1998. Synaptic targets of pyramidal neurons providing intrinsic horizontal connections in monkey prefrontal cortex. *J. Comp. Neurol.* 390 (2), 211–224.
- Morrison, A., Mehring, C., Geisel, T., Aertsen, A., Diesmann, M., 2005. Advancing the boundaries of high connectivity network simulation with distributed computing. *Neural Comput.* 17 (8), 1776–1801.
- Mooser, F., Bosking, W.H., Fitzpatrick, D., 2004. A morphological basis for orientation tuning in primary visual cortex. *Nat. Neurosci.* 7 (8), 872–879.
- Morishima, M., Kawaguchi, Y., 2006. Recurrent connection patterns of corticostriatal pyramidal cells in frontal cortex. *J. Neurosci.* 26 (16), 4394–4405.
- Newman, M.E.J., 2003. The structure and function of complex networks. *SIAM Rev.* 45 (2), 167–256.
- Nathanson, J.L., Yanagawa, Y., Obata, K., Callaway, E.M., 2009. Preferential labeling of inhibitory and excitatory cortical neurons by endogenous tropism of adeno-associated virus and lentivirus vectors. *Neuroscience* 161, 441–450.
- Ojima, H., Honda, C.N., Jones, E.G., 1991. Patterns of axon collateralization of identified supragranular pyramidal neurons in the cat auditory cortex. *Cereb. Cortex* 1, 80–94.
- Ojima, H., Takayanagi, M., 2004. Cortical convergence from different frequency domains in the cat primary auditory cortex. *Neuroscience* 126, 203–212.
- Peters, A., Kara, D.J., Harriman, K.M., 1981. The neuronal composition of area 17 of rat visual cortex. III. Numerical considerations. *J. Comp. Neurol.* 238, 263–275.
- Pucak, M.L., Levitt, J.B., Lund, J.S., Lewis, D.A., 1996. Patterns of intrinsic and associational circuitry in monkey prefrontal cortex. *J. Comp. Neurol.* 376, 614–630.
- Ramón y Cajal, S., 1911. *Histologie du Système Nerveux de l'Homme et des Vertébrés*, Translated by L. Azoulay, Maloine, Paris.
- Read, H.L., Winer, J.A., Schreiner, C.E., 2001. Modular organization of intrinsic connections associated with spectral tuning in cat auditory cortex. *Proc. Natl. Acad. Sci. U.S.A.* 98 (14), 8042–8047.
- Rockland, K.S., Lund, J.S., Humphrey, A.L., 1982. Anatomical binding of intrinsic connections in striate cortex of tree shrews (*Tupaia glis*). *J. Comp. Neurol.* 209, 41–58.
- Rockland, K.S., Lund, J.S., 1983. Intrinsic laminar lattice connections in primate visual cortex. *J. Comp. Neurol.* 216, 303–318.
- Rockland, K.S., Virga, A., 1989. Terminal arbors of individual “feedback” axons projecting from area V2 to V1 in the macaque monkey: A study using immunohistochemistry of anterogradely transported phaseolus vulgaris-leucoagglutinin. *J. Comp. Neurol.* 285 (1), 54–72.
- Rockland, K.S., Virga, A., 1990. Organization of individual axons projecting from area V1 (area17) to V2 (area 18) in the macaque monkey. *Vis. Neurosci.* 4, 11–28.
- Rockland, K.S., 1995. Morphology of individual axons projecting from area V2 to MT in the macaque. *J. Comp. Neurol.* 355 (1), 15–26.
- Rockland, K.S., Knutson, T., 2000. Feedback connections from area MT of the squirrel monkey to areas V1 and V2. *J. Comp. Neurol.* 425, 345–368.
- Rockland, K.S., Knutson, T., 2001. Axon collaterals of meynert cells diverge over large portions of area V1 in the macaque monkey. *J. Comp. Neurol.* 441, 134–147.
- Rockland, K.S., 2002. Visual cortical organization at the single axon level: a beginning. *Neurosci. Res.* 42, 155–166.
- Rockland, K.S., 2004a. Feedback connections: Splitting the Arrow. In: Collins, C., Kaas, J.H. (Eds.), *The Primate Visual System*. CRC Press, pp. 387–405.
- Rockland, K.S., 2004b. Connectional neuroanatomy: the changing scene. *Brain Res.* 1000 (1–2), 60–63.
- Rumberger, A., Tyler, C.J., Lund, J.S., 2001. Intra- and inter-areal connectivity between the primary visual cortex V1 and the area immediately surrounding V1 in the rat. *Neuroscience* 102, 35–52.
- Schmidt, K.E., Löwel, S., 2002. Long-range intrinsic connections in cat primary visual cortex. In: Payne, B., Peters, A. (Eds.), *The Cat Primary Visual Cortex*. Academic Press, p. 387.
- Shmuel, A., Korman, M., Sterkin, A., Harel, M., Ullman, S., Malach, R., Grinvald, A., 2005. Retinotopic specificity and selective clustering of feedback projections from V2 to V1 in the owl monkey. *J. Neurosci.* 25 (8), 2117–2131.
- Schüz, A., Braitenberg, V., 2002. The human cortical white matter: Quantitative aspects of cortico-cortical long-range connectivity. In: Schüz, A., Miller, R. (Eds.), *Cortical Areas: Unity and Diversity*. Taylor and Francis, pp. 377–385.
- Schüz, A., Chaimow, D., Liewald, D., 2005. Quantitative aspects of corticocortical connections: A tracer study in the mouse. *Cereb. Cortex* 16, 1474–1486.
- Schüz, A., Palm, G., 1989. Density of neurons and synapses in the cerebral cortex of the mouse. *J. Comp. Neurol.* 286, 442–455.
- Sincich, L.C., Blasdel, G.G., 2001. Oriented axon projections in primary visual cortex of the monkey. *J. Neurosci.* 21 (12), 4416–4426.
- Sporns, O., Zwi, D.Z., 2004. The small world of the cerebral cortex. *Neuroinformatics* 2, 145–162.
- Stepanyants, A., Hirsch, J., Martinez, L.M., Kisvárdy, Z.F., Ferecsko, A.S., Chklovskii, D.B., 2007. Local potential connectivity in cat primary visual cortex. *Cereb. Cortex* 18 (1), 13–28.
- Stepanyants, A., Martinez, L.M., Ferecsko, A.S., Kisvárdy, Z.F., 2009. The fractions of short- and long-range connections in the visual cortex. *PNAS* 106 (9), 3555–3560.
- Stettler, D., Das, A., Bennet, J., Gilbert, C., 2002. Lateral connectivity and contextual interactions in macaque primary visual cortex. *Neuron* 36, 739–750.
- Tanigawa, H., Wang, Q., Fujita, I., 2005. Organization of horizontal axons in the inferior temporal cortex and primary visual cortex of the macaque monkey. *Cereb. Cortex* 15, 1887–1899.
- Thomson, A.M., Bannister, P., 2003. Interlaminar connections in the neocortex. *Cereb. Cortex* 13, 5–14.
- Tootell, R.B.H., Silverman, M.S., Hamilton, S.L., Switkes, E., De Valois, R.L., 1988. Functional anatomy of Macaque striate cortex. V. Spatial frequency. *J. Neurosci.* 8 (5), 1610–1624.
- Ts'o, D.Y., Frostig, R.D., Lieke, E.E., Grinvald, A., 1990. Functional organization of the primate visual cortex revealed by high resolution optical imaging. *Science, New Series* 249 (4967), 417–420.
- Tyler, C., Dunlop, S., Lund, R., Harman, A., Dann, J., Beazley, L., Lund, J., 1998. Anatomical comparison of the macaque and marsupial visual cortex: Common features that may reflect retention of essential cortical elements. *J. Comp. Neurol.* 400, 449–468.
- Van Hooser, S.D., Heimel, J.A., Chung, S., Nelson, S.N., 2006. Lack of patchy horizontal connectivity in primary visual cortex of a mammal without orientation maps. *J. Neurosci.* 26 (29), 7680–7692.
- van Vreeswijk, C., Sompolinsky, H., 1996. Chaos in neuronal networks with balanced excitatory and inhibitory activity. *Science* 274, 1724–1726.
- van Vreeswijk, C., Sompolinsky, H., 1998. Chaotic balanced state in a model of cortical circuits. *Neural Comput.* 10, 1321–1371.
- Voges, N., Aertsen, A., Rotter, S., 2007. Statistical analysis of spatially embedded networks: From grid to random node positions. *Neurocomputing* 70 (10–12), 1833–1837.
- Voges, N., Perrinet, L., 2010. Phase space analysis of networks based on biologically realistic parameters. *J. Physiol. Paris* 104 (1–2), 51–60.
- Voges, N., Guijarro, C., Aertsen, A., Rotter, S., 2010. Models of cortical networks with long-range patchy projections. *J. Comput. Neurosci.* 28 (1), 137–154.
- Wallace, M.N., Bajwa, S., 1991. Patchy intrinsic connections of the ferret primary auditory cortex. *NeuroReport* 2, 417–420.
- Wallace, M.N., Kitzes, L.M., Jones, E.G., 1991. Intrinsic inter- and intralaminar connections and their relationship to the tonotopic map in cat primary auditory cortex. *Exp. Brain Res.* 86 (3), 527–544.
- Wickersham, I.R., Finke, S., Conzelmann, K.-K., Callaway, E.M., 2007. Retrograde neuronal tracing with a deletion-mutant rabies virus. *Nat. Methods* 4 (1), 47–49.
- Yabuta, N.H., Callaway, E.M., 1998. Cytochrome-oxidase blobs and intrinsic horizontal connections of layer 2/3 pyramidal neurons in primate V1. *Vis. Neurosci.* 15 (6), 1007–1027.
- Yoshimura, Y., Sato, H., Imamura, K., Watanabe, Y., 2000. Properties of horizontal and vertical inputs to pyramidal cells in the superficial layers of the cat visual cortex. *J. Neurosci.* 20 (5), 1931–1940.
- Yoshimura, Y., Callaway, E., 2005. Fine-scale specificity of cortical networks depends on inhibitory cell type and connectivity. *Nat. Neurosci.* 8 (11), 1552–1559.
- Yoshioka, T., Levitt, J.B., Lund, J.S., 1992. Intrinsic lattice connections of macaque monkey visual cortical area V4. *J. Neurosci.* 12, 2785–2802.
- Yoshioka, T., Blasdel, G.G., Levitt, J.B., Lund, J.S., 1996. Relation between patterns of intrinsic lateral connectivity, ocular dominance and cytochrome oxidase-reactive regions in macaque monkey striate cortex. *Cereb. Cortex* 6, 297–310.
- Yousef, T., Bonhoeffer, T., Kim, D.-S., Eysel, U.T., Toth, E., Kisvárdy, Z.F., 1999. Orientation topography of layer 4 lateral networks revealed by optical imaging in cat visual cortex (area 18). *Eur. J. Neurosci.* 11, 4291–4308.